A FINITE ELEMENT APPROACH FOR CALCULATING THE WAVE ATTENUATION CHARACTERISTICS OF EPOXY POLYMER MATRIX COMPOSITES

by

Pratik Prashant Ghag

A thesis submitted to the faculty of
The University of North Carolina at Charlotte
in partial fulfillment of the requirements
for the degree of Master of Science in
Mechanical Engineering

Charlotte

2017

Approved by:

Dr. Alireza Tabarraei

Dr. Ronald Smelser

Dr. Vincent Ogunro

ABSTRACT

PRATIK PRASHANT GHAG. A finite element approach for calculating the wave attenuation characteristics of epoxy polymer matrix composites. (Under the direction of DR. ALIREZA TABARRAEI)

The macroscopic properties of a polymer composite are significantly affected by the properties of the inclusions, size, shape, and distribution. Finite element (FE) modeling provides a viable approach for investigating the effects of the inclusions on the macroscopic properties of the polymer composite. In this thesis, we use the finite element method to investigate ultrasonic wave propagation in polymer matrix composite with a dispersed phase of inclusions. The finite element models are made up of three phases; viz. the polymer matrix, inclusions (micro constituent), and interphase zones between the inclusions and the polymer matrix. The interphase zone is explicitly modeled to study the effect of the properties of the interphase on the polymer composite. The analysis is performed on a three dimensional finite element model and the attenuation characteristics of ultrasonic longitudinal waves in the matrix are evaluated. The analysis is performed using the finite element code ABAQUS. We investigate the attenuation in the polymer composite by changing the size, volume fraction of inclusions, and interphase material properties. The effect of interphase properties like the Young's modulus and the thickness of the interphase layer on the wave attenuation characteristics of the polymer composite are studied by conducting a sensitivity analysis. The effect of loading frequency of the wave on the attenuation characteristics are also studied by varying the frequency in the range of 1 - 4 MHz.

Results of the test revealed that a higher volume fraction of inclusions gave higher attenuation in the polymer composite compared to the lower volume fraction model. Smaller size inclusions are preferred over larger sizes as they give higher wave attenuation. It was found that the attenuation characteristics of the polymer composite are

better at higher frequencies compared to lower frequencies. It is also concluded that the arrangement of inclusions in a polymer composite plays a significant role in the attenuation characteristics of the composite. The Young's modulus and the thickness of the interphase layer also play a vital role in the wave attenuation characteristics.

ACKNOWLEDGEMENTS

I would first like to thank Dr.Alireza Tabarraei who gave me an opportunity to work in his research group. His support and help throughout the research period inspired to me learn new things for the successful completion of this work. I also take this opportunity to thank Dr.Ronald Smelser and Dr.Vincent Ogunro for agreeing to serve on my thesis committee. I would like to thank the professors of the Mechanical Engineering and Engineering Science Department at UNC Charlotte for sharing their knowledge and guiding me through the completion of my degree program. I also thank the Mechanical Engineering and Engineering Science Department at UNC Charlotte for providing me the resources needed for the research and for continued assistance until the end of this research.

I thank all my seniors and colleagues who guided me and helped me during my research. I especially thank my family and friends in India and the United States for encouraging me to pursue my degree. Their support, both financially and morally, has been very important to me. Lastly, I would like to thank the Graduate School at UNC Charlotte for providing me with financial assistance through an assistantship for the period of this research.

DEDICATION

To my family who encouraged me, my teachers who guided me, and my friends who supported me.

TABLE OF CONTENTS

LIST OF FIGURES

LIST OF TABLES

CHAPTER 1: INTRODUCTION

Polymer like epoxy, polyurea have limited industrial applications on their own as their mechanical properties are not as high as metals. However, when a different component in the form of inclusions is added to a polymer matrix to form a composite, the resulting polymer matrix composite can have exceptional mechanical properties. The inclusions can be spherical or cylindrical shapes. The materials used for inclusions are glass, carbon nanotubes, etc. The advantage of the composite material is that it has the properties of both of it's components. High strengths and stiffnesses, ease of moulding complex shapes, high environmental resistances coupled with low densities, make the resultant composite superior to metals in many applications.

The inclusions are embedded in the matrix to make the matrix stronger. The composites are strong and light, for example they are often stronger than steel and weigh much less. These properties of the composites are used by automobile manufactures to make vehicles lighter and thus much more fuel efficient. Such desirable properties of the polymer composites have attracted wide attention in their usage in applications such as aerospace, automobile, and shipping industries. Many applications of the polymer composites include components which are subjected to dynamic loads which may include automobile components like bumpers, dashboards, airplane parts and ship components. The wide spectrum of applications makes it necessary to study the dynamic behavior of the polymer composites.

Polymers like polyurea, epoxy have excellent attenuation properties as a results of which they are extensively used for coating purposes which can help in absorbing the incident waves. This property of the polymers is used to create coatings for military applications like helmets, tanks, vehicles, police vehicles, equipments, places with high

security risks such as bridges, chemical tanks, government buildings, storage areas, etc.

Several studies have been performed in the past to study the mechanical properties of polymer composites. Llorca and Segurado [1] studied three types of composite materials: rigid spheres and spherical voids in elastic matrix and elastic spheres (glass inclusions) in an elastic matrix (epoxy resin). Mechanical properties like elastic, shear and bulk modulus and Poisson's ratio were determined at different volume fractions for the polymer composites. These were compared with the results obtained with three classical analytical models: the Mori-Tanaka mean field analysis, the generalized self-consistent method, and Torquato's third order approximation. The results show an increase in the elastic, shear, and bulk moduli as the volume fraction of the inclusions increases which is found to be in close agreement with the classical methods at lower volume fractions.

Wave propagation through the polymer composites is one of the important dynamic properties for the applications mentioned earlier in this chapter as such applications are often subjected to shock waves. The propagation of periodic and transient waves is complicated in polymer composites as there is scattering of waves from the material interfaces and due to dissipation in the matrix [2]. The wave propagation through the polymer composites is greatly influenced by the addition of micro-inclusions. The wave speed and amplitude are affected by the shape, size, and distribution of the inclusions in the polymer matrix [2].

Biwa et al. [3] carried out numerical analyses for longitudinal wave attenuation in a glass-epoxy composite and a rubber-particle toughened poly(methyl methacrylate) (PMMA) blend. In the former, the attenuation is due to scattering by particles and by absorption in the matrix; while in the latter, attenuation is additionally caused by absorption in particles. Biwa studied the viscoelastic properties of the matrix and their influence on the scattering characteristics and absorption of the waves. The

results were compared with the classical Rayleigh scattering behavior. The inter-particle distance along with the reflections from the neighboring particles play an important role in wave attenuation at higher volume fractions. Biwa et al. studied the influence of frequency and particle radius on the scattering, absorption and resulting attenuation characteristics. The attenuation coefficients of longitudinal and transverse waves in these polymers are shown in Fig 1.1 at different frequencies. It is observed from the figure that the attenuation coefficients show an almost linear dependency with frequency as is observed for solid polymers [4, 5].

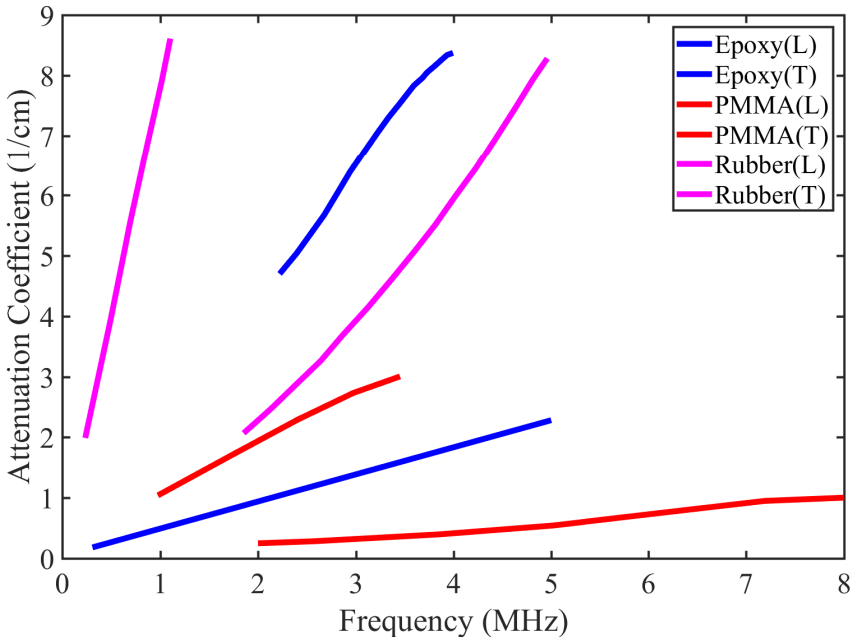

Figure 1.1: Frequency-dependent attenuation co-efficients of Longitudinal (L) and transverse (T) waves in epoxy [6], PMMA [7] and rubber (from assumed complex moduli).

Kim [8] conducted a comparative study on eight existing theoretical models to create some benchmark results for wave propagation in two-dimensional composite materials. The models include Waterman and Truell [9], Llyod and Berry [10], Varadan et al. [11], Kanaun and Levin [12], Sabina and Willis [13], Kim [14], Beltzer and Brauner [15], and Yang and Mal [16]. He conducted numerical calculations for

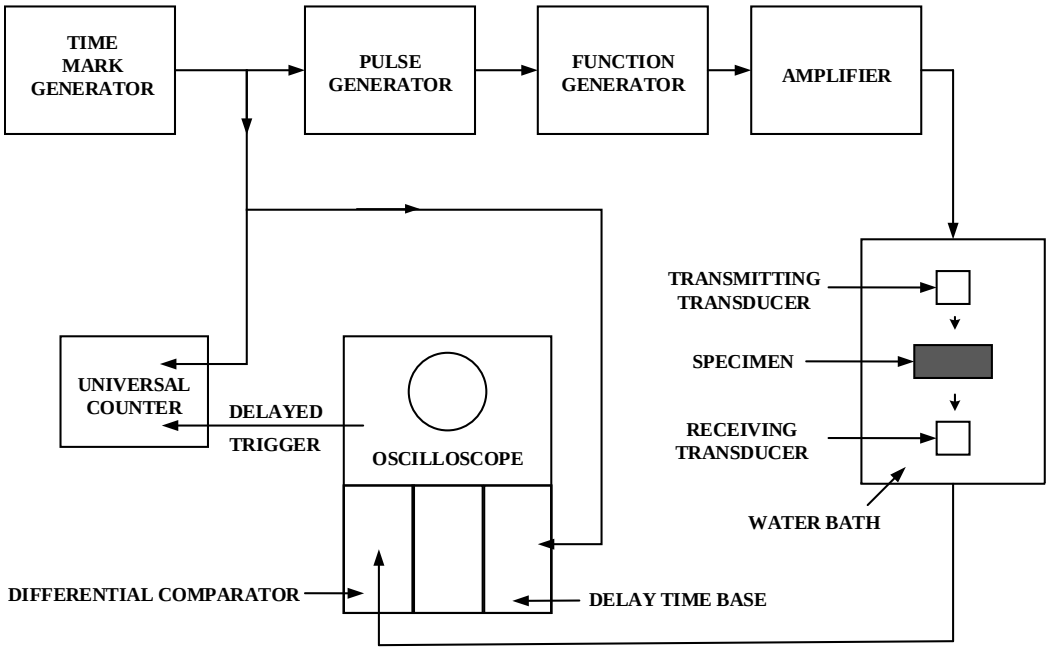

Figure 1.2: Experimental setup to measure attenuation and phase velocities [17].

different composites by varying the material properties, volume concentration of the micro-inclusions, and the loading frequency. He also discussed the effects of micro-inclusions on the wave attenuation characteristics. In his studies he concluded that whenever the point scattering approximation is relevant, the Llyod and Berry [10] model was more accurate than the Waterman and Truell [9] model. He further reported that the Kim [14] and Kanaun and Levin [12] models predict values close to each other possibly because they were based on a common hypothesis and do not exhibit failure in all the cases considered. He reported that as the attenuation is more sensitive to the composite's microstructure, the disagreements in calculation of the wave attenuation is due to difference in the microstructures assumed in these different models.

Kinra et al. [17] studied ultrasonic wave propagation through an epoxy-glass composite by conducting experiments in a frequency range of 0.3 - 5 MHz by varying the volume fraction of glass from 8.6 % to 53 %. The composite studied in the experiment consists of spheres of glass dispersed in a random homogeneous manner in an

epoxy. He measured the longitudinal and shear wave phase velocities and the attenuation of the longitudinal waves over the specified frequency. The experimental setup is shown in Fig 1.2. An ultrasonic pulse is applied using the pulse generator which when fed to the function generator produces a tone burst of the desired frequency. This frequency and given to the transmitting transducer. The specimen is stored in a distilled water bath. The ultrasonic sound is applied through the water coupling, and the output wave is collected by the receiving transducer which is then displayed on the oscilloscope. The results of the experiments show that the attenuation increases as the frequency of the wave is increased. Kinra reported higher volume fractions of the inclusion yields better attenuation at lower frequencies.

The disadvantage of using an experiment is the lack of flexibility in the test models as a large number of specimens are to be generated to study the effect of different sizes, shapes and volume fraction of the inclusions which can be difficult to manufacture. The finite element technique provides another technique to study the attenuation characteristics of the polymer composite.

Liu et al. [2] studied the wave propagation in polymer composite using the extended finite element method (XFEM). They studied the effect of volume fraction and loading frequency on the wave attenuation characteristics of the polymer composite with spherical and cylindrical inclusions. The wave attenuation characteristics are studied for two volume fractions and three orientations in the case of cylindrical inclusions. The results are compared to the theoretical and experimental results in the frequency range of 1 - 4 MHz. In the case of spherical inclusions, the results were in good agreement with the experimental and analytical results for lower volume fractions, while at higher volume fractions only at lower frequencies. In the case of cylindrical inclusions, results showed maximum attenuation when the inclusions were oriented in the direction of loading. They also reported an increase in attenuation as the loading frequency is increased.

Another important aspect that plays a vital role in the wave attenuation characteristics of the polymer composite is the interphase region. Interphase region is formed due to cross-linking or crystallization between the polymer matrix and the inclusion. Interphase region can be formed due to mechanical imperfections, unreacted polymer components, fiber treatments, restricted macromolecular mobility due to the fiber surface, and other inconsistencies [18–20]. The interphase region is depicted in Fig 2.3. The thickness of the interphase region depends upon the material bonding properties [21]. Many efforts have been made to study the characteristics of the interphase. Techniques like nanoindentation, nano-scratch and Atomic Force microscopy (AFM) are used to study the properties and thickness of the interphase. An explicit study of the interphase region is essential as the region is considered to be one of the weakest regions in the polymer composite. It has been reported that the structural integrity and modes of failure for the polymer composites is dependent on the properties and the thickness of the interphase [21].

In this thesis, we study the attenuation characteristics of a polymer composite by using finite element modeling. Elastic inclusions are randomly dispersed in a polymer matrix with linear viscoelastic material properties. The effect of interphase properties on the wave attenuation characteristics is studied. Interphase is a region which has been ignored in the studies that have been conducted on this material in the past. The modeling of the interphase is very difficult as the thickness is very thin and the material properties lie with the properties of the polymer matrix and the inclusions. As a result of the uncertainty of the material properties, sensitivity analysis is performed to take into account the effect on the attenuation characteristics of the polymer composite. The impact of size and volume fraction of the inclusion and loading frequencies on wave attenuation is investigated. In Chapter 2, the thesis problem and the approach used to solve the problem is described. The details about the finite element model and various algorithms used to define the finite element

model are described in Chapter 3. The description of the material model and their constitutive models for three phases, viz. the polymer matrix, inclusions, and the interphase, are presented in Chapter 4. The results of the analysis and their discussion are found in Chapter 5. Chapter 6 concludes the thesis and presents the scope for future work.

CHAPTER 2: THESIS PROBLEM AND APPROACH

In this chapter, the thesis problem and the approach used to solve the problem are presented.

2.1 Thesis Problem

In this thesis, we use the finite element method to investigate the ultrasonic wave propagation in polymer matrix composite (PMC). The polymer composite has a dispersed phase of inclusions intended to improve the mechanical properties. Since the macroscopic properties of a composite are affected by the inclusion size, shape and distribution, we evaluate the effect these parameters on the wave attenuation characteristics of polymer composite. Furthermore, we investigate the role of interphase and loading frequency on the attenuation of waves in polymer composite. The goal is to gain fundamental insights on designing polymer composite with high attenuation capabilities.

2.2 Approach

This study is conducted using commercial finite element code ABAQUS (Dassault Systèmes, Inc). The finite element analysis are conducted using three dimensional finite element models. The inclusions are dispersed randomly in the polymer matrix. A viscoelastic material model is used to model the polymer matrix and linear elastic material model is used for inclusions. The details of the finite element model and material model are given in chapters 3 and 4, respectively.

A schematic diagram of the model used in the analysis is shown in Figure 2.1. As shown, a uniform sinusoidal pressure with amplitude P_o = 10 MPa, and frequency of f = 1-4 MHz is applied at the surface at z = 2.0 mm along the Z direction. The

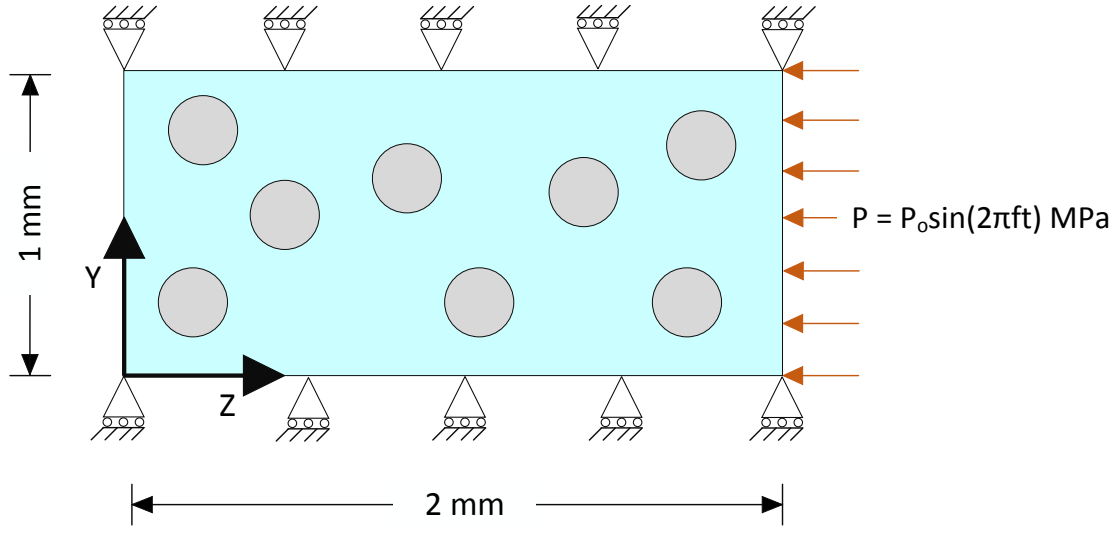

Figure 2.1: Schematic of the finite element model.

surface at z = 0.0 is free while a one-dimensional impact is stimulated by fixing the other surfaces in the X and Y directions.

The element data for all the time steps are recorded for all the simulations at z = 2.0 mm and z = 0.5 mm as shown in the Figure 2.2. The time history plot for stress σ_{zz} (in the loading direction) is generated using the history data at these surfaces. The surface at z = 2.0 mm is expected to give the same stress amplitude as the input wave, i.e. 10 MPa. The amplitude of the wave reduces as it travels through the matrix due to scattering and reflections from the inclusions and material damping of the polymer matrix. The attenuation coefficient (α) is calculated using [2]

$$\alpha = \frac{\ln(\frac{S_1}{S_2})}{(z_1 - z_2)} \tag{2.1}$$

Where,

z_1 = 2 mm,

z_2 = 0.5 mm,

S_1 - Stress at z_1 (MPa) and

S_2 - Stress at z_2 (MPa).

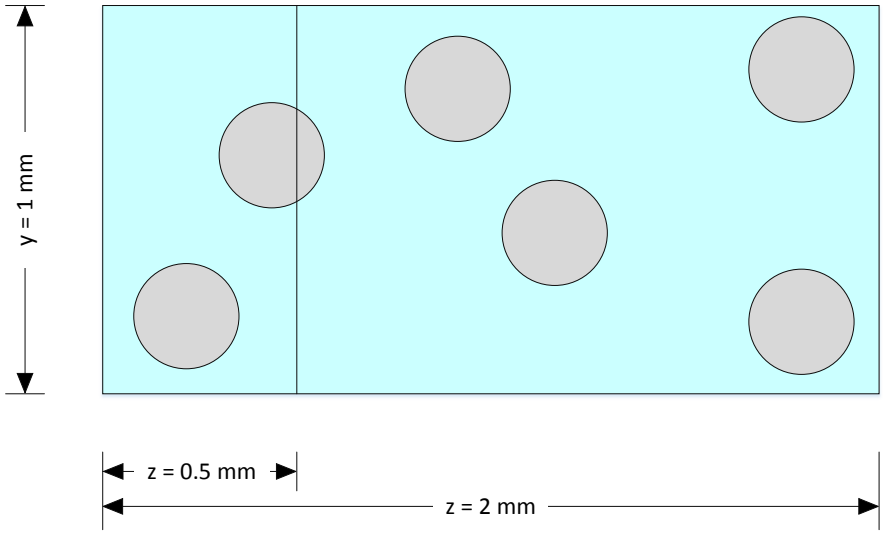

Figure 2.2: Schematic of the surfaces where the results are recorded.

2.3 Design Parameters to study

In this thesis, the impact of shape, size and distribution of inclusions on the attenuation characteristics of polymer composite are studied. The details of the finite element models used to study the effect of each of these parameters are provided.

2.3.1 Effect of the volume fraction

The volume fraction is defined as the ratio of the volume of the inclusions to the total volume of the composite. In this study, we build several finite element models of polymer composites with various inclusion volume fractions. The finite element simulations are carried out at constant radii of the spherical inclusions, polymer matrix dimensions and interphase size. The simulations are conducted to evaluate the effect of the volume fraction on the attenuation of the wave. The details of the composite configuration used are shown in Table 2.1, Table 2.2 and Table 2.3.

2.3.2 Effect of the loading frequency

The finite element simulations are conducted to evaluate the effect of the loading frequency on the attenuation characteristics of the polymer composite. The loading

Table 2.1: Finite element models to evaluate the effect of volume fraction of spherical inclusions with radius 120μm on wave attenuation.

Finite element model	Radius of inclusion(μm)	Volume fraction(%)	Number of inclusions
1	120	5	10
2	120	8.6	18
3	120	12	25
4	120	15	31
5	120	20	41

Table 2.2: Finite element models to evaluate the effect of volume fraction of spherical inclusions with radius 150μm on wave attenuation.

Finite element model	Radius of inclusion(μm)	Volume fraction(%)	Number of inclusions
1	150	5	5
2	150	8.6	9
3	150	12	13
4	150	15	16
5	150	20	21

Table 2.3: Finite element models to evaluate the effect of volume fraction of spherical inclusions with radius 180μm on wave attenuation.

Finite element model	Radius of inclusion(μm)	Volume fraction(%)	Number of inclusions
1	180	5	3
2	180	8.6	5
3	180	12	7
4	180	15	9
5	180	20	12

frequency is varied in the range of 1-4 MHz while all the other design parameters remain constant throughout the simulations.

2.3.3 Effect of the size of inclusions

For this study we built finite element models with different radii of spherical inclusions, while other parameters like polymer matrix dimensions, volume fraction, and interphase size are kept constant. The loading frequency is varied in the range between 1-4 MHz. The details of the study are shown in the Table 2.4.

Table 2.4: Finite element models to evaluate the effect of size of spherical inclusions on wave attenuation.

Finite element model	Radius of inclusion(μm)	Volume fraction(%)	Number of inclusions
1	120	5	10
2	150	5	5
3	180	5	3
4	120	8.6	18
5	150	8.6	9
6	180	8.6	5
7	120	12	25
8	150	12	13
9	180	12	7
10	120	15	31
11	150	15	16
12	180	15	9
13	120	20	41
14	150	20	21
15	180	20	12

2.3.4 Effect of the interphase properties

The molecular layers responsible for the adhesion between the inclusion and polymer matrix is defined as the interphase. Interphase layer in the polymer composite is shown in Figure 2.3. Interphases play a significant role in the global properties of the nanocomposites [22–25]. In this study, we analyze the effect of stiffness and thickness of the interphase region on the attenuation characteristics of the polymer composite. The stiffness of the interphase is varied between the stiffness of the polymer matrix and the stiffness of the inclusions. The polymer matrix dimensions, size of inclusions, and volume fraction are kept constant in these simulations.

2.3.5 Effect of arrangement of inclusions

The arrangement of inclusions also affect the attenuation characteristics of the wave in polymer composite. The effect of arrangement of the inclusions is studied by conducting simulations of the finite element models with different arrangement

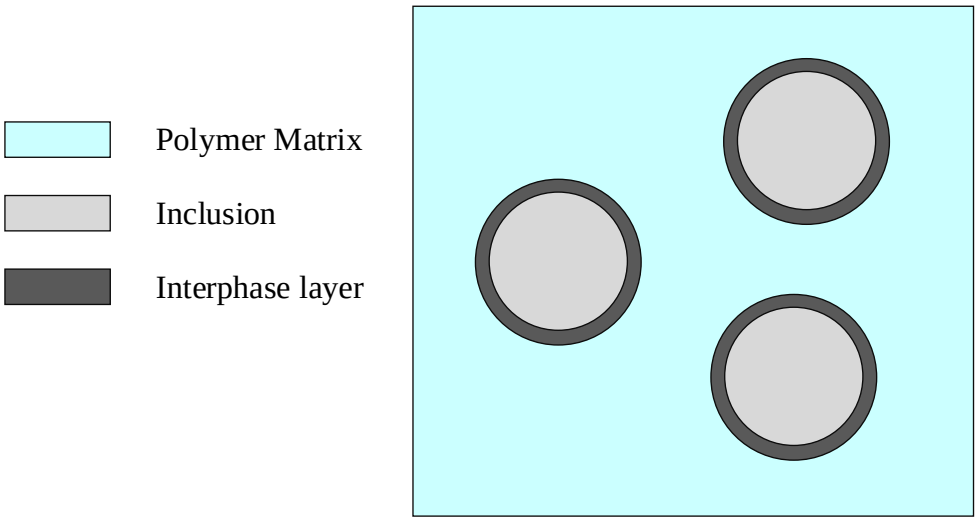

Figure 2.3: Schematic illustration of the PMC with interphase layer.

of inclusions which is achieved with the help of randomization by Python scripting [26]. A detailed description of the arrangement of inclusions with Python scripting is provided in Chapter 3. A number of iterations are carried out at the same conditions to evaluate the effect of arrangement of inclusions within the polymer matrix.

CHAPTER 3: FINITE ELEMENT MODELING

In this study, we carry out finite element analysis (FEA) on polymer composite by considering a simple cuboid geometry. The inclusions are randomly dispersed in the matrix and separated by some minimum distance from each other. The details of the geometry, forces, constraints and finite element model are given in the following sections.

3.1 Finite element model generation algorithm

There are number of techniques which are used for the generation of computational finite element models. Random sequential absorption (RSA) algorithm [27–30] prevents the occurrence of overlapping inclusions by requiring that any new potential candidate inclusion does not overlap with previously accepted inclusions. This is done by random generation of size, location and orientation of the inclusions. In this process, the current volume is updated continuously as each new inclusion gets added, and the process continues till the desired volume fraction is achieved or the number of attempts exceeds the predefined limit. The technique has limitation in achieving high volume fractions (>50%) due to jamming issue. Another method of finite element model generation is the Monte Carlo (MC) [31–33] technique which is a two-step scheme. In the first step all the filler particles or the inclusions are deposited in the simulation box then in the second step the location and orientation of the inclusions is changed randomly until the desired volume fraction is achieved. The removal of overlaps is slow in the MC technique as the movements are random. Molecular dynamic based process [34, 35] are used to accelerate the removal of overlaps.

For the purpose of this research a modified version of RSA algorithm is used for the

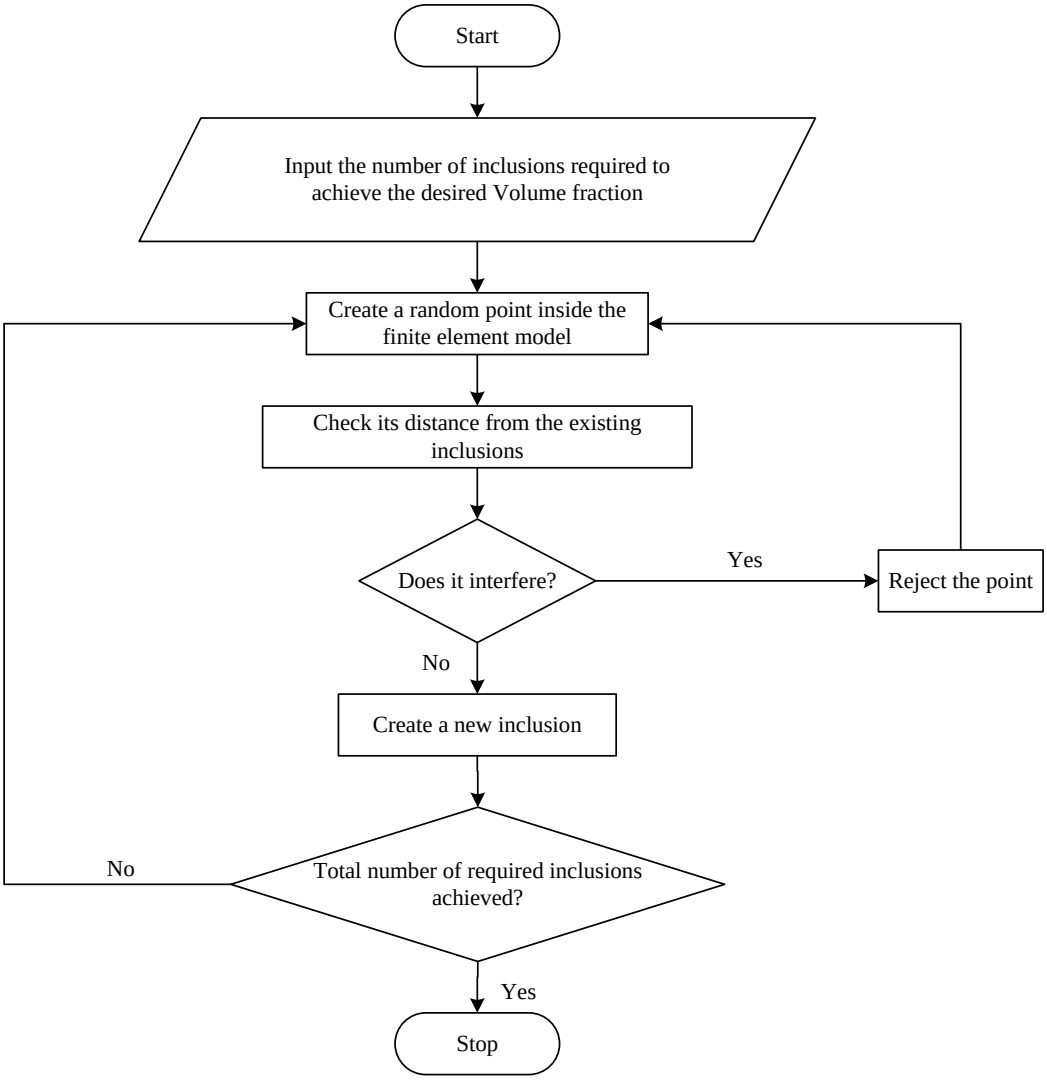

Figure 3.1: Flowchart for finite element model generation algorithm.

generation of inclusions by employing Python scripting in Abaqus [26]. We specify the number of inclusions required to achieve the desired volume fraction. The volume fraction is defined as the ratio of the volume of the inclusions to the total volume of the composite. The volume fraction c is varied between 5% to 20% to study its effect on attenuation characteristics of polymer matrix. For this study, the inclusions are dispersed only in the geometry of $1 \times 1 \times 1.5$ mm^3 since we are recording the data at z = 0.5 mm as shown in the Figure 2.2. The number of inclusions n required to

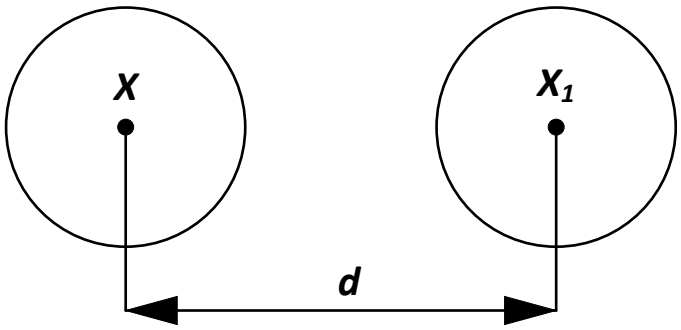

Figure 3.2: Distance between any two inclusions at any given time.

achieve the desired volume fraction is determined as follows:

$$n \approx \frac{c \times V}{v} \tag{3.1}$$

Where,

n - Number of inclusions,

c - Volume fraction,

V - Total volume and

v - Volume of the inclusion.

Location of the inclusion is generated by random number generation in Python. The point generated in Python serves as the center point of the inclusion. The distance of this point is checked with any point previously accepted by the algorithm to ensure there is no overlap between the inclusions. The distance d between any two inclusions is shown in Figure 3.2. The distance between the two points is determined as follows:

$$d = \sqrt{(x - x_1)^2 + (y - y_1)^2 + (z - z_1)^2} \tag{3.2}$$

Where,

d - Distance between two points,

x - X coordinate of the accepted inclusion,

y - Y coordinate of the accepted inclusion,

z - Z coordinate of the accepted inclusion,

x_1 - X coordinate of the candidate inclusion,

y_1 - Y coordinate of the candidate inclusion and

z_1 - Z coordinate of the candidate inclusion.

A minimum gap of 12.5 % of radius is maintained between the inclusions to ensure proper meshing of the finite element model. This distance is utilized in the finite element model only to ensure proper meshing of the model as in reality the inclusions can be in contact or very close with one another . But as this would create difficulty in meshing the finite element model a minimum distance separating the inclusions was used in the algorithm. Figure 3.1 shows the graphical representation of the RSA algorithm in the form of a flow-chart. The process continues until the required number of inclusions to satisfy the volume fraction are achieved.

3.2 Finite element model

We conduct simulations on three-dimensional polymer composites with spherical inclusions. An example of three-dimensional finite element model is shown is Figure 3.3.

The geometry of the specimen used in the simulation is a $1 \times 1 \times 2$ mm^3 cuboid as shown in Figure 3.3, the inclusions are generated by the modified RSA algorithm as described in Section 3.1. The inclusions are modeled as solid spheres. The radius of the inclusions varies from 120μm to 180μm as specified in Section 2.3.3.

The polymer matrix is meshed using tetrahedral elements with an average size of 0.05 mm. The inclusions are meshed using hexahedral elements with a mesh size of 0.05 mm. In the case of studies involving the interphase the inclusions as well as the interphase are meshed with tetrahedral elements with a mesh size of 0.025 mm and the polymer matrix is meshed with tetrahedral elements with a mesh size of 0.05

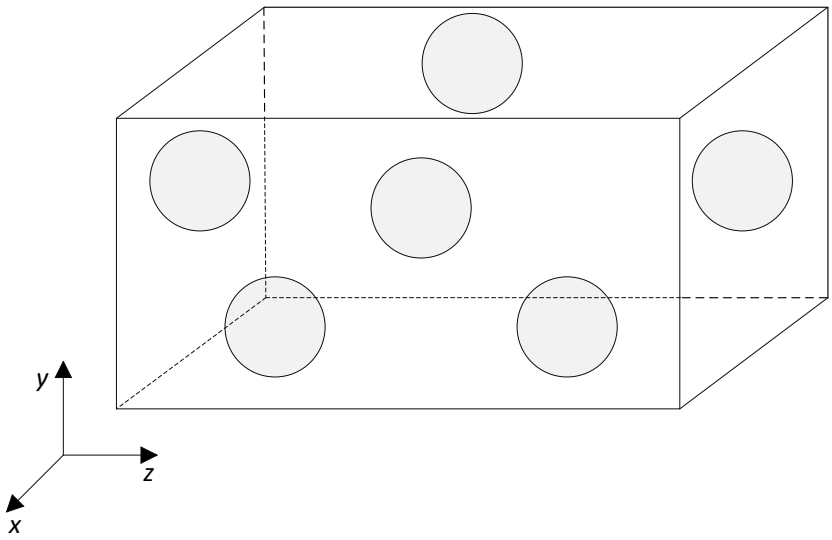

Figure 3.3: Representation of finite element model with spherical inclusions.

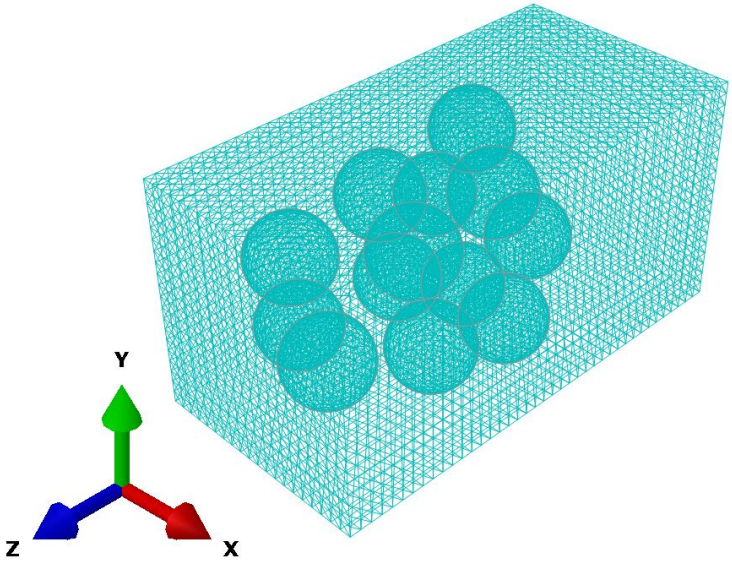

Figure 3.4: Representation of meshed finite element model for 12% volume fraction.

mm. A node to node connectivity is maintained in all phases of the model. Figure 3.4 shows the meshed model for PMC with inclusions as well as the interphase. From the Abaqus element library tetrahedral C3D10 elements and hexahedral C3D20 elements are used for the finite element simulations.

To increase the accuracy of the simulations, full integration method is used for both of the element types. The elements and their integration points are shown in Figure

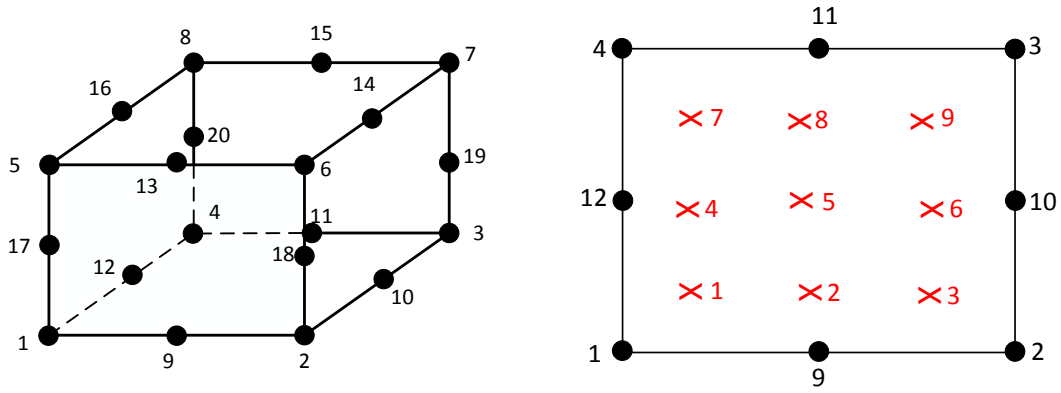

(a) C3D20 (b) C3D20

Figure 3.5: C3D20 element with nodes and integration points [26].

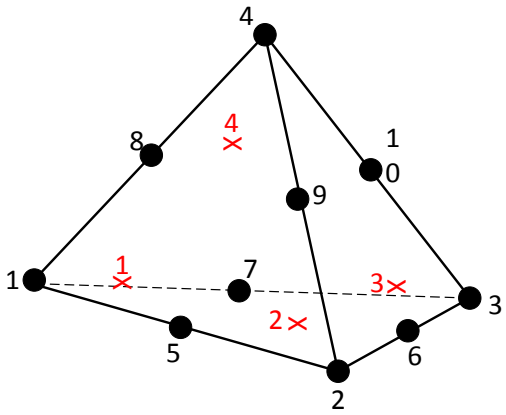

Figure 3.6: C3D10 element with nodes and integration points [26].

5.18.

3.3 Forces and Constraints

Linear displacement boundary conditions, uniform traction boundary conditions and periodic boundary conditions are some of the boundary conditions which are used in computational mechanics procedures [36]. For the purpose of this study we use linear displacement boundary conditions. A uniform sinusoidal compressive pressure with P_o = 10 MPa is applied at the surface z = 2 mm as shown in Figure 2.1. All other surfaces are constrained in two translational degrees of freedom in the

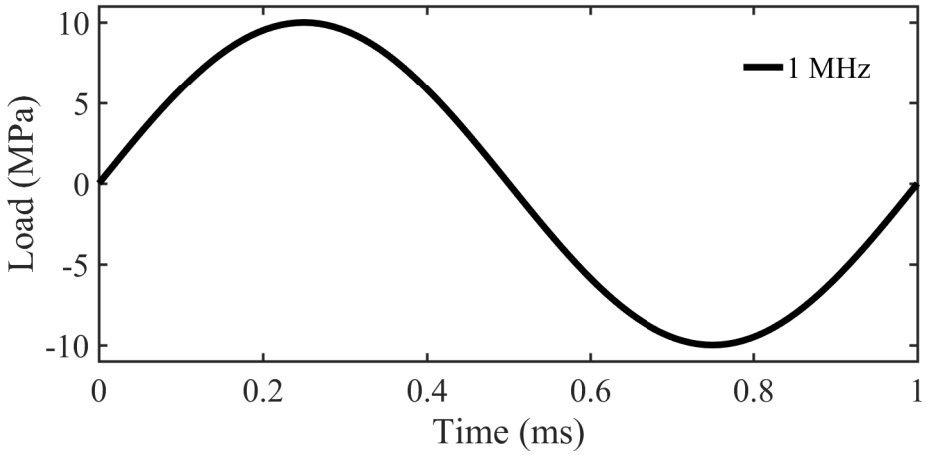

Figure 3.7: Sinusoidal loading curve for frequency = 1 MHz.

X and Y direction. Translational motion is allowed in the direction of loading i.e. the Z direction. A node set is created on a plane at z = 0.5 mm where the readings for output are recorded. The sinusoidal pressure P is given as follows:

$$P = P_o \sin(2\pi f t) \tag{3.3}$$

Where,

P_o = 10 MPa,

f - Frequency (MHz) and

t - Time (ms).

The load verses time curve for 1 MHz frequency loading is shown in Figure 3.7. For the purpose of this study the frequency is varied between 1 MHz to 4 MHz while the force amplitude P_o remains the same for all finite element solutions.

CHAPTER 4: CONSTITUTIVE MATERIAL MODELS

Constitutive models play a vital role in the accuracy of the finite element analysis. In physics and engineering, a constitutive equation is a relation between any two parameters or physical quantities which helps to predict the material behavior when it is subjected to external forces. A very good example of the constitutive equation would be the Hooke's law (stress-strain relation). Most metals exhibit linearly elastic behavior and the Hooke's law can be used to predict the material behavior.

In this study, the glass spheres (inclusions) and the interphase are considered linear elastic while a linear viscoelastic material model is chosen for the epoxy matrix. The material models are studied in detail in the subsequent sections.

4.1 Polymer matrix (Epoxy)

The polymer matrix considered in this thesis is an epoxy. There are many applications for epoxy-based materials which includes coatings, adhesives and composite materials such as those involving carbon fiber and fiberglass reinforcements. The cured polymers can be produced with a wide range of properties because of the chemistry of the epoxies and range of commercially available variations. Epoxy is known for its excellent adhesion, chemical and thermal resistance, good mechanical properties and very good electrical insulating properties.

Epoxy is used in paints and coatings which are often used in industrial and automotive applications since they are more heat resistant than latex-based and alkyd-based paints. Epoxy adhesives are high-performance adhesives of a part of the class of adhesives called "structural adhesives" or "engineering adhesives" which are used in the construction of aircrafts, bicycles, boats, skis, snowboards, and other applications

which involve high strength bonds.

The concept of viscoelasticity, the constitutive viscoelastic model for the polymer matrix and the material parameters are described in the following sections.

4.1.1 Viscoelasticity

Viscoelasticity is the property of materials which exhibit both viscous and elastic characteristics when undergoing deformation. Whenever a material is subjected to an external force, internal forces are created in the material to resist the force due to distortion in the physical structure. The nature of the internal forces depend on the type of the material on which the external force is applied. For example, in the case of metals, the internal forces are created due the inter-atomic forces while in the case of fluids like oil or air, the internal forces are due to rapid movement of the molecules in the medium [37]. Viscoelastic materials exhibit a combined behavior of these elastic and viscous materials. Combination of such behavior is observed in materials like soil, polymers, concrete, and biological tissues [37].

Viscoelastic materials can be modeled in order to determine their stress and strain or force and displacement interactions. Viscoelastic behavior has elastic and viscous components modeled as linear combinations of spring and dampers which can be combined in a variety of arrangements to produce a simulated viscoelastic response [38]. An example of these models would be the Maxwell fluid model and the Kelvin solid model. The models are explained in detail later in the chapter. The two types of responses which are observed in viscoelastic materials are the stress relaxation and creep. Stress relaxation is the reduction in stress at a constant strain. The creep is increase in strain at a constant stress [38]. The stress relaxation response will thus be useful for us to define the viscoelastic response because strains will be calculated in finite element analysis from the nodal displacements which can be used for evaluation of stress using the stress relaxation equation.

4.1.1.1 Maxwell fluid model

Consider the Maxwell fluid model shown in Figure 4.1. An equation between stress and strain can be obtained for any mechanical model using equilibrium and kinematic equations for the system and constitutive equations for the elements. For the model, equilibrium gives,

$$\sigma = \sigma_s = \sigma_d \tag{4.1}$$

where σ is the applied stress, σ_s is the stress in the spring and σ_d is the stress in the damper. From the kinematic condition, we have,

$$\varepsilon = \varepsilon_s + \varepsilon_d \tag{4.2}$$

where ε is the total strain in the Maxwell element, ε_s is the strain in the spring while ε_d is the strain in the damper. The constitutive equations are,

$$\sigma_s = E\varepsilon_s = \sigma \tag{4.3}$$

differentiating,

$$\dot{\sigma} = E\dot{\varepsilon_s} \tag{4.4}$$

and

$$\sigma_d = \mu\frac{d\varepsilon_d}{dt} = \mu\dot{\varepsilon_d} = \sigma \tag{4.5}$$

Differentiating Eq 4.2, we have,

$$\dot{\varepsilon} = \dot{\varepsilon_s} + \dot{\varepsilon_d} \tag{4.6}$$

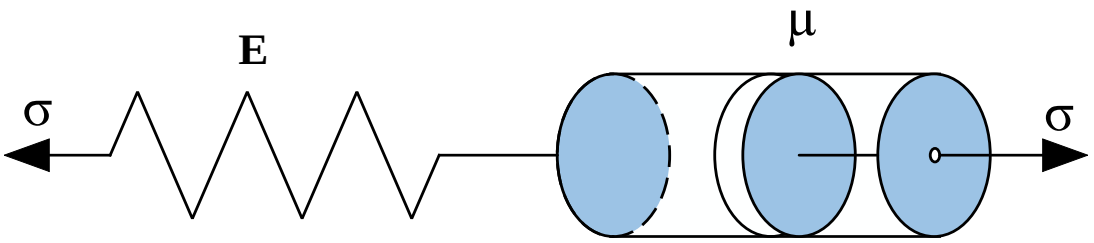

Figure 4.1: Maxwell fluid model.

Now, subsituting Eq 4.4 and 4.5 into Eq 4.6, we have,

$$\dot{\sigma} + \frac{E}{\mu}\sigma = E\dot{\varepsilon} \tag{4.7}$$

Rearranging, we have,

$$\sigma + \frac{\mu}{E}\dot{\sigma} = \mu\dot{\varepsilon} \tag{4.8}$$

or

$$\sigma + p_1\dot{\sigma} = q_1\dot{\varepsilon} \tag{4.9}$$

The relaxation time is defined as the inverse of the co-efficient of the stress rate,

$$\tau = \frac{\mu}{E} \tag{4.10}$$

As described in section 4.1.1, for the case of creep, the applied stress is constant and can be written as,

$$\sigma(t) = \sigma_0 M(t) \tag{4.11}$$

where $M(t)$ is the Heavyside function and is defined as,

$$\begin{aligned} M(t) &= 1 \quad for \quad t > 0 \\ M(t) &= 0 \quad for \quad t < 0 \end{aligned} \tag{4.12}$$

$$\begin{aligned} M(t) &= 1 \quad for \quad t > 0 \\ M(t) &= 0 \quad for \quad t < 0 \end{aligned} \tag{4.13}$$

Thus, the stress is constant for time greater than zero. Now, the Eq 4.7 for the case of creep, the solution is,

$$\varepsilon(t) = \sigma_0 \left(\frac{1}{E} + \frac{1}{\mu} \right) \tag{4.14}$$

or

$$\varepsilon(t) = \sigma_0 Q(t) \tag{4.15}$$

where

$$Q(t) = \left(\frac{1}{E} + \frac{1}{\mu} \right) \tag{4.16}$$

is the creep compliance.

The creep and creep recovery behavior for a Maxwell fluid is shown in Fig 4.2. In the creep test, the model is subjected to a constant stress as described earlier. Then as a result of the free spring, the model would have a sudden increase in strain as shown in the Fig 4.2. An equally important facet of the constant stress test is to evaluate the strain variation when the stress is removed. This is known as the creep recovery test and is also shown in the Fig 4.2. As seen in the figure once the stress is removed the strain falls to a value ε_p remaining constant there after.

In the stress relaxation test as discussed in section 4.1.1, the stress is studied at a constant strain. The solution for Eq. 4.7 for relaxation is obtained using a step input in strain,

$$\varepsilon(t) = \varepsilon_0 M(t) \tag{4.17}$$

with a resulting stress output of,

$$\sigma(t) = \varepsilon_0 E e^{\frac{-t}{\tau}} \tag{4.18}$$

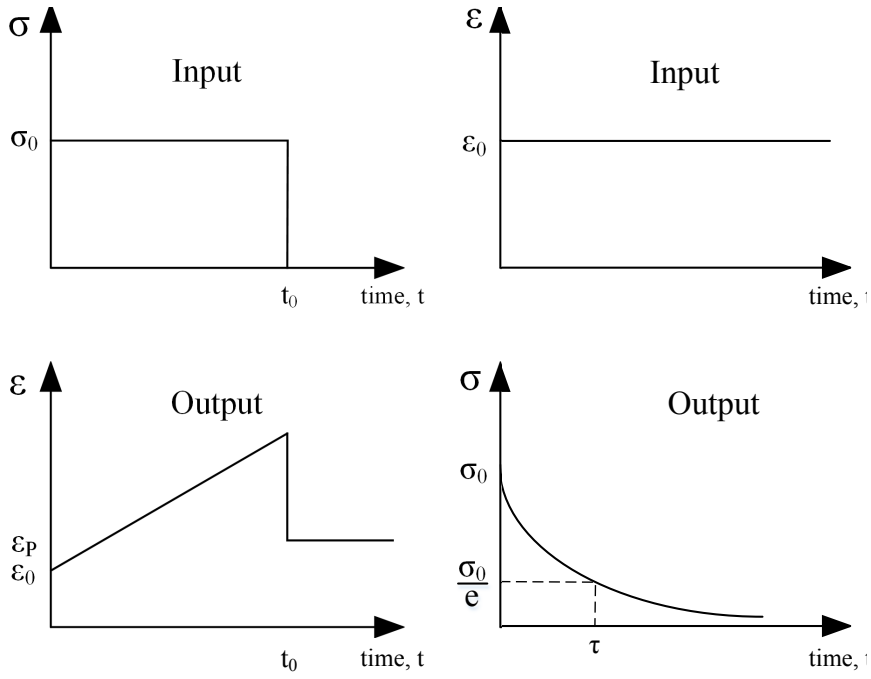

Figure 4.2: Creep, creep recovery and relaxation response of Maxwell fluid.

where

$$E(t) = Ee^{\frac{-t}{\tau}} \tag{4.19}$$

is the relaxation modulus. The relaxation behavior for the Maxwell fluid is shown in Fig 4.2. As seen in the figure for a constant strain, the stress gradually decreases as less stress is required to maintain the strain.

The deformation mechanisms associated with relaxation and creep are related to the long chain molecular structure of the polymer. In creep, the continuous loading gradually induces strain accumulation as the polymer molecules rotate and unwind to accommodate the load. Similarly, during relaxation at a constant strain, the initial sudden strain occurs more rapidly than can be accommodated by the molecular structure. The molecules will again rotate and unwind as a result of which less stress is needed to maintain the same strain level [38].

4.1.1.2 Kelvin solid model

The Kelvin solid model is shown in Fig 4.3. The equilibrium equation is,

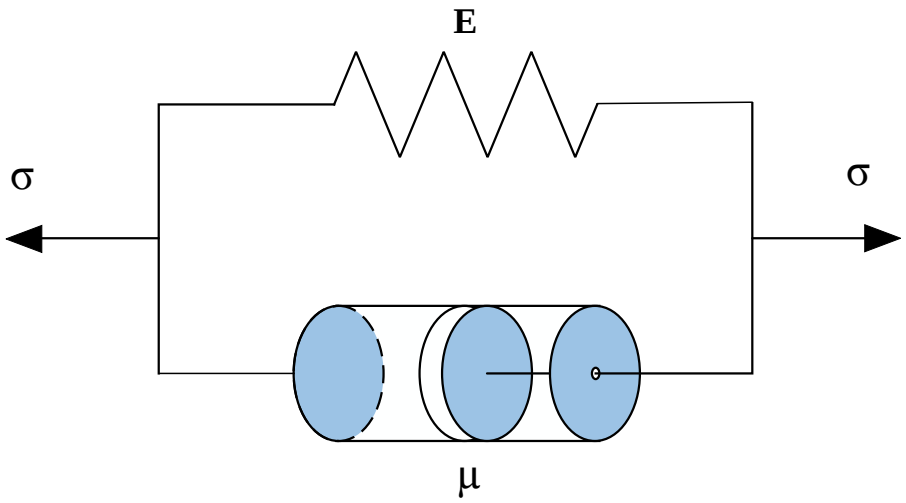

Figure 4.3: Kelvin solid model.

$$\sigma = \sigma_s + \sigma_d \tag{4.20}$$

and the kinematic condition is,

$$\varepsilon = \varepsilon_s = \varepsilon_d \tag{4.21}$$

The constitutive equations are,

$$\begin{aligned} \sigma_s &= E\varepsilon_s \\ \sigma_d &= \mu\dot{\varepsilon_d} \end{aligned} \tag{4.22}$$

and the differential equation becomes,

$$\sigma = E\varepsilon + \mu\dot{\varepsilon} \tag{4.23}$$

Under the creep loading the solution becomes,

$$\varepsilon(t) = \frac{\sigma_0}{E}\left(1 - e^{\frac{-t}{\tau}}\right) \tag{4.24}$$

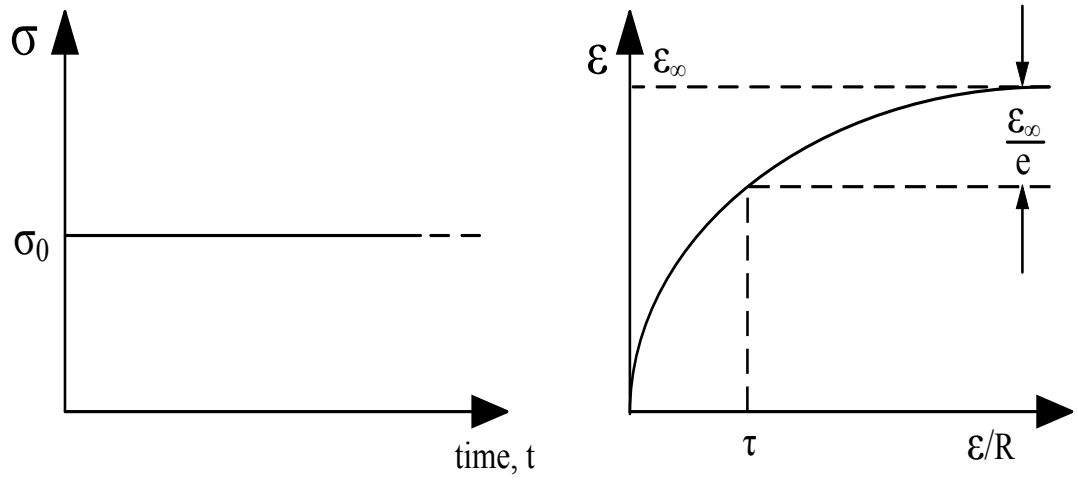

Figure 4.4: Creep of a Kelvin solid model.

and the creep compliance is,

$$Q(t) = \frac{1}{E}\left(1 - e^{\frac{-t}{\tau}}\right) \tag{4.25}$$

The creep response of the Kelvin solid model is illustrated in Fig 4.4.

As the damper only allows the spring to move slowly with time, there is no initial elasticity and the model is not useful in understanding the relaxation response of materials as the damper does nor allow the spring to move instantaneously [38].

4.1.2 Material Parameters for Epoxy matrix

The stress relaxation modulus $G(t)$ is defined by a Prony series expansion,

$$G(t) = G_0\left(1 - \sum_{i=1}^{n} g_i\left(1 - e^{\frac{-t}{\tau_i}}\right)\right) \tag{4.26}$$

where G_0 is the instantaneous shear modulus and g_i and τ_i are material constants defined in Table 4.1 taken from [2]. The temperature effects were not considered for defining the model. The viscosity of the bulk modulus κ is neglected.

Table 4.1: Prony series parameters for Epoxy matrix

g_i	τ_i
0.0738	463.4
0.1470	0.06407
0.3134	0.0001163
0.3786	7.321e-7

Table 4.2: Material parameters for Epoxy matrix

G_0 (MPa)	1481.80
E_0 (MPa)	4060.11
κ (MPa)	5205.00
ρ (g/cm^3)	1.18
ν	0.37

The other input parameters for this material like G_0, instantaneous Young's modulus E_0, κ, density ρ and poisson's ratio ν are given in Table 4.2.

4.2 Inclusions (Glass)

The inclusions for the study are made from glass. The glass inclusions are much stiffer and stronger than the polymer matrix. A linear elastic model is used for modeling the inclusions whose response can be defined using Hooke's law which is given by,

$$\sigma_{ij} = C_{ijkl}\varepsilon_{kl} \tag{4.27}$$

where, C_{ijkl} is the elastic modulus.

The material is assumed to be isotropic i.e. the material properties are constant in all the directions. The glass inclusions are assumed to have a Young's modulus E of 64890.0 MPa, Poisson's ratio ν of 0.249 and a density ρ of 2.47 g/cm^3.

4.3 Interphase

The interphase is modeled as a linear elastic material. In reality the interphase should be modeled as a linear viscoelastic material. But the material parameters for

the viscoelasticity were not available for the interphase and hence, a linear elastic material was chosen. The objective being to study the attenuation due to scattering from the surfaces of the inclusions and not due dissipation due to viscoelastic nature of the interphase. The research aims to study the elastic moduli of the interphase and its effect on the wave attenuation of the polymer composite. A sensitivity analysis (SA) is performed to evaluate the effect on the wave attenuation characteristics due to uncertainty in the input parameters for the interphase. The focus for this part of the study was to evaluate the effect of thickness and the Young's modulus of the interphase on the wave attenuation characteristics of the polymer composite. Hence, the thickness and Young's modulus of the interphase were considered as the stochastic inputs for the study. The Poisson's ratio is assumed to be 0.249 and the density ρ of the interphase is assumed to be 1.18 g/cm^3 which is the mean of the densities for the inclusion and the polymer matrix.

4.3.1 Design of Experiments (DoE)

A number of schemes like the deterministic sampling, random sampling, stratified sampling have been devised in the past to scan the design space of the input variables [39–41]. Deterministic sampling involves samples at regular intervals which usually increases the number samples exponentially with increasing dimension which is not efficient when the cost of each realisation is high. An alternative to this would be the random sampling which overcomes the disadvantage. Mont Carlo Simulation (MCS) is a common approach based on random independent sampling in the given design space. The disadvantage of MCS is that the approach can lead to artificial correlations in the input and output parameters [39]. To overcome the issue of undesired correlations, stratified sampling has been developed. In this method, the sampling space is divided into number of separate groups called strata and random samples are picked from each strata. This is further improved with Latin Hypercube sampling (LHS) in which range of each variable is divided into equal intervals and a sample

is selected from each interval [41]. In this study, LHS is used to generate random values for Young's Modulus and thickness of the interphase to overcome undesired correlations between input parameters.

4.3.2 Sensitivity Analysis

The sensitivity analysis is conducted by preparing finite element models with different material properties. For each volume fraction 25 samples for 2 variables were generated using lhsdesign function of MATLAB [42] and for each sample 25 finite element models are generated to take into account the effect of randomness of the positioning of the inclusions. The Young's modulus of the interphase is chosen in the range of 14.0 GPa to 51.0 GPa and the thickness is chosen in the range of 15 μm to 30 μm.

CHAPTER 5: RESULTS AND DISCUSSION

In this section we compute results for parameters affecting the mechanical properties of the polymer matrix composites. The analysis results were post processed using commercial finite element post processing tool ABAQUS (Dassault Systèmes, Inc). Time history data for stress σ_{zz} values was collected at planes specified in section 2.2 and was plotted against time to study the stress wave propagation. Then the wave attenuation co-efficient is calculated using Eq 2.1 by considering the peak value of the stresses on both the planes as specified above. For the case of this study the following parameters are evaluated as specified in section 2.3 and the results of each of the these parameters are discussed in the subsequent sections:

1. Effect of volume fraction
2. Effect of loading frequency
3. Effect of size of inclusions
4. Effect of interphase material properties.

5.1 Validation

To validate that the procedure for this research, the results from the FEM were plotted in Figure 5.1 with published theoretical predictions [3] and results obtained using extended finite element method (XFEM) [2]. As can be seen from the figure the FEM results are very close to the Analytical and XFEM results. Simulations were also performed in which the matrix material was replaced by the inclusion material (glass) without any inclusions to see the effect of elastic material on the wave attenuation of the polymer composite. No attenuation was observed in these simulations which proves that the attenuation occurs only by scattering from the surface of the

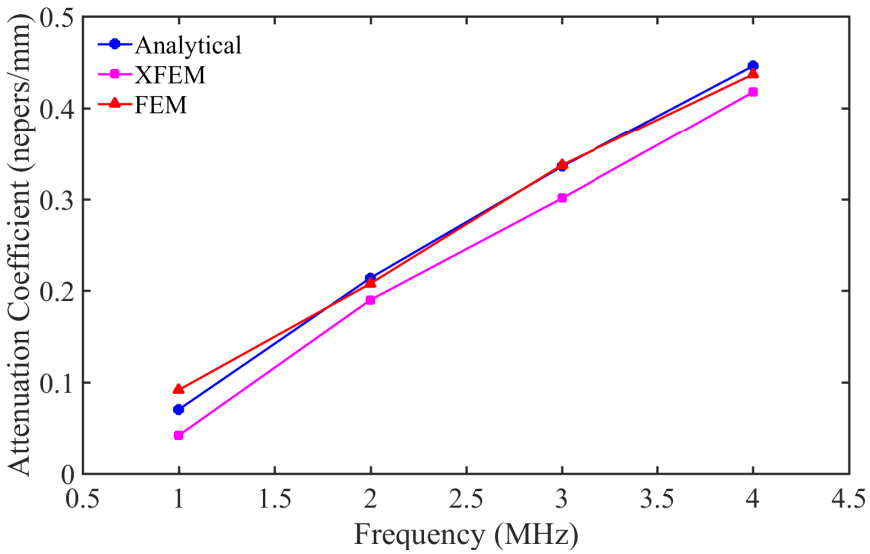

Figure 5.1: Attenuation in the particulate composite with volume fraction 0.086 vs frequency.

inclusions.

5.2 Ensemble averaging

The process used to generate finite element model has been described in detail in section 3.1. As specified in the section, the location of the inclusions is achieved by random number generation using Python scripting. As the position of the inclusion plays an important role in determining the mechanical properties of polymer matrix composite, ensemble averaging was performed to remove the effect of randomness of the positioning of the inclusions. Accordingly, the following saturation criteria should be met:

$$\left| \frac{\langle \alpha \rangle^{2J} - \langle \alpha \rangle^{J}}{\langle \alpha \rangle^{2J}} \right| < Tol \tag{5.1}$$

where $\langle\ \rangle^{J}$ implies an ensemble average using j realisations, and $\langle\ \rangle^{2J}$ represent the same quantity obtained using twice this number of realisations. The accuracy of the operation is determined by the convergence tolerance for ensemble averaging specified by Tol in the above equation. A 5% polymer matrix composite was used to

conduct ensemble averaging test for simplification of the procedure. Figure 5.2 shows the ensemble averaging test conducted for 5% polymer matrix composite against the number of realisations. It can be deduced from the figure that convergence would be guaranteed for 50 realisations with a convergence error of less that 0.7 %. As a result of this test, 50 iterations where performed for each design parameter mentioned in section 2.3 to remove the effect of randomness of the positioning of the inclusions.

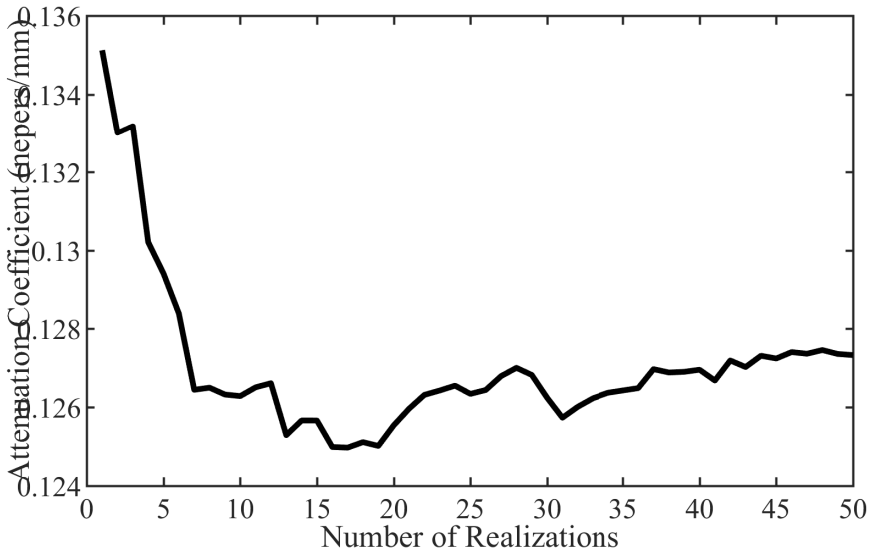

Figure 5.2: The average of the attenuation co-efficient (α) for 5% PMC verses the realization number.

5.3 Effect of volume fraction

Volume fraction is one of the vital factors which affects the properties and behavior of the polymer matrix composite. To evaluate the effect of volume fraction on the wave attenuation a number of finite element simulations where performed by changing the number of inclusions while keeping the radius of the inclusion constant. These simulations were performed with parameters mentioned in section 2.3.1.

Figures 5.3, 5.4 and 5.5 show the effect on attenuation of the wave due to change in volume fraction when the radius of the inclusion is 120 μm, 150 μm and 180 μm respectively for frequencies ranging from 1 MHz to 4 MHz. As can be seen from the

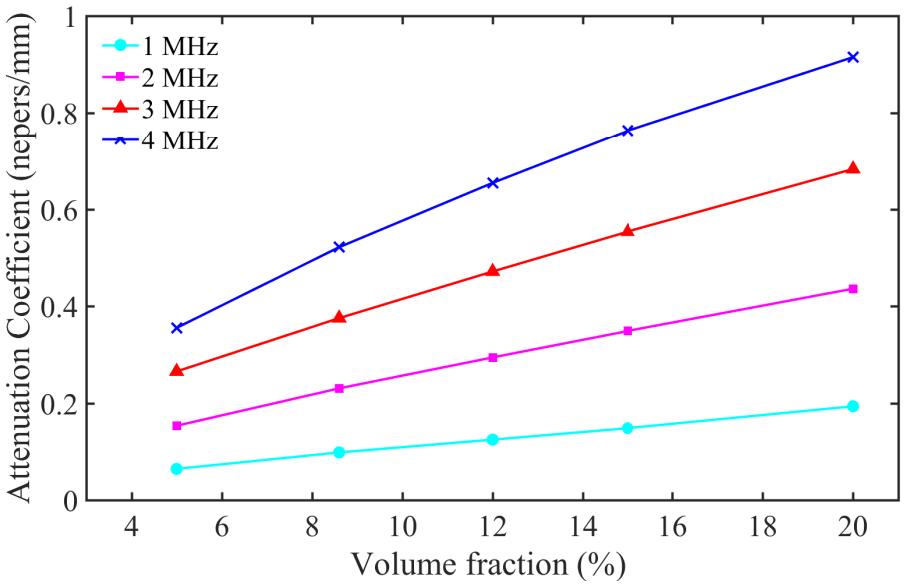

Figure 5.3: Attenuation Coefficient v/s Volume fraction for inclusion radius 120 μm for different frequencies.

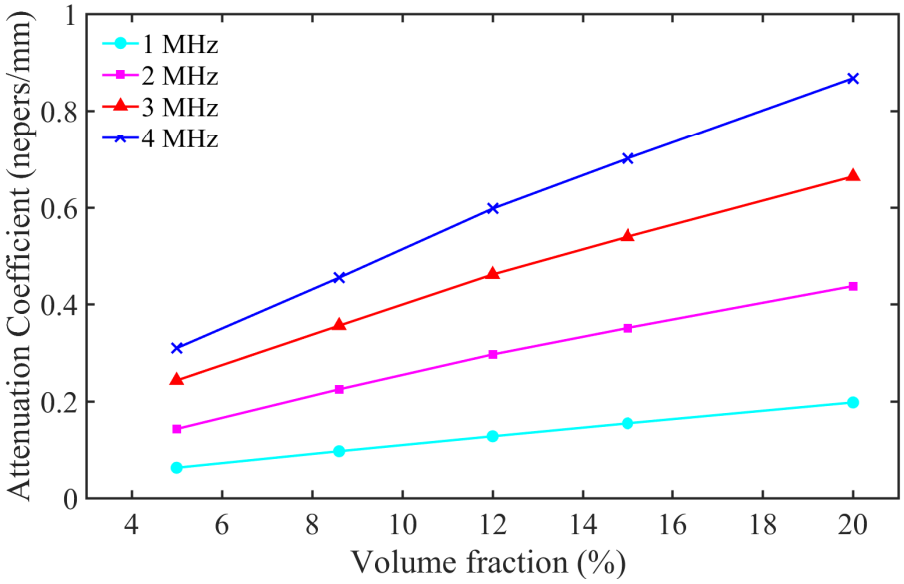

Figure 5.4: Attenuation Coefficient v/s Volume fraction for inclusion radius 150 μm for different frequencies.

figures, the attenuation of the wave increases as the volume fraction increases. Due to higher number of inclusions in higher volume fractions the scattering of the waves are higher. The stress dissipation is higher because of more scattering at higher volume fractions resulting in more attenuation. It is also observed from the figures that

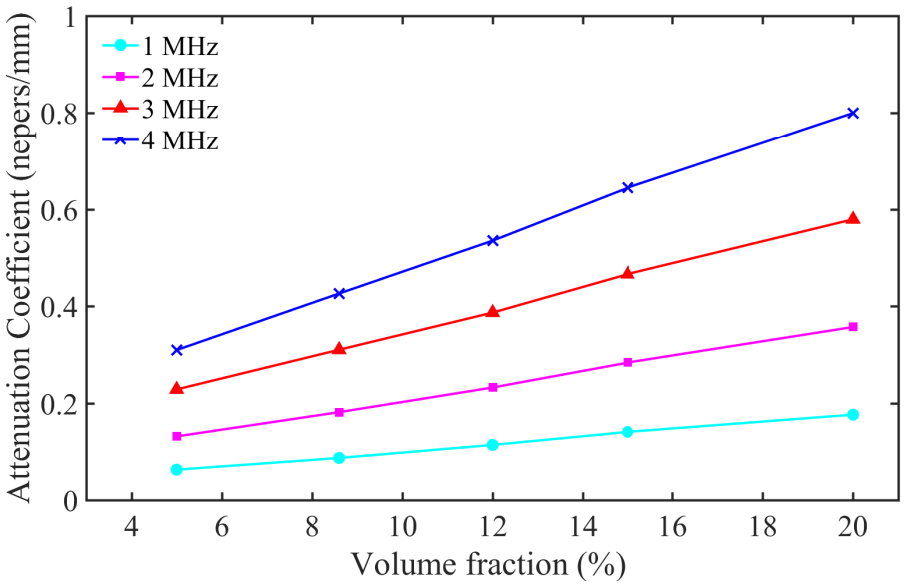

Figure 5.5: Attenuation Coefficient v/s Volume fraction for inclusion radius 180 μm for different frequencies.

the attenuation improves substantially for higher frequencies as the volume fraction increases.

5.4 Effect of loading frequency

The attenuation characteristics are observed to change with change in frequency. To study this, finite element simulations were performed with change in frequency from 1 MHz to 4 MHz with all other parameters remaining constant. The simulations were conducted on radius ranging from 120 μm to 180 μm with volume fraction from 5% to 20%. The time history of surface averaged stress σ_{zz} at surfaces z = 2 mm and z = 0.5 mm are shown in Figure 5.6 for 5% volume fraction. We can find peaks of the stress σ_{zz} at z = 0.5 mm decrease compared to that at z = 2 mm. This is a result of scattering by by the inclusions and absorption by the matrix. It is also observed that the decrease grows strongly with increasing of frequency [2].

Figures 5.7, 5.8 and 5.9 show the effect on loading frequency on the wave attenuation for radius 120 μm, 150 μm and 180 μm respectively for volume fraction ranging from 5% to 20%. It also shows the attenuation characteristics for the epoxy matrix

in the absence of inclusions.

From the results, it can be seen that the attenuation co-efficients at lower frequencies are far less sensitive to the volume fraction, and close to that of the epoxy matrix [2]. It is also observed that at frequencies greater than 2 MHz, at higher volume fractions the curves get separated from each other i.e. the attenuation co-efficients are sensitive to the volume fraction. So, higher the volume fraction (number of inclusions) higher is the attenuation observed.

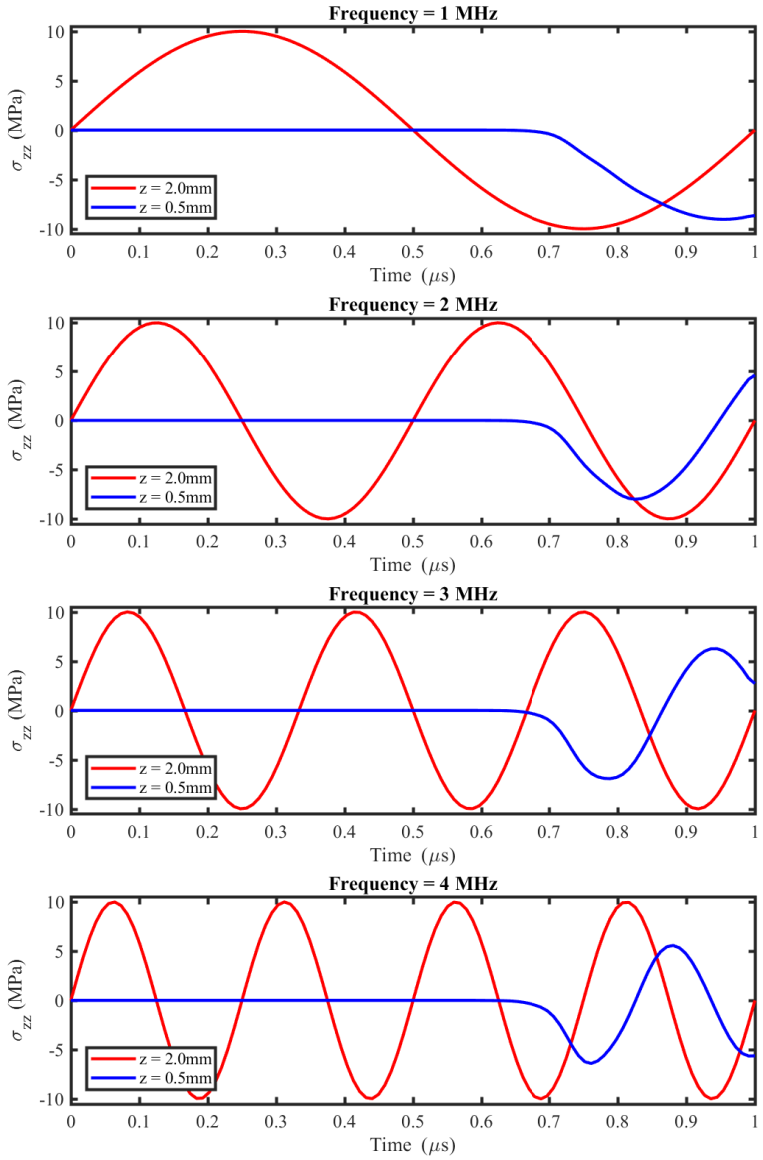

Figure 5.6: Time history of surface averaged stress σ_{zz} at z = 2 mm and z = 0.5 mm at different frequencies.

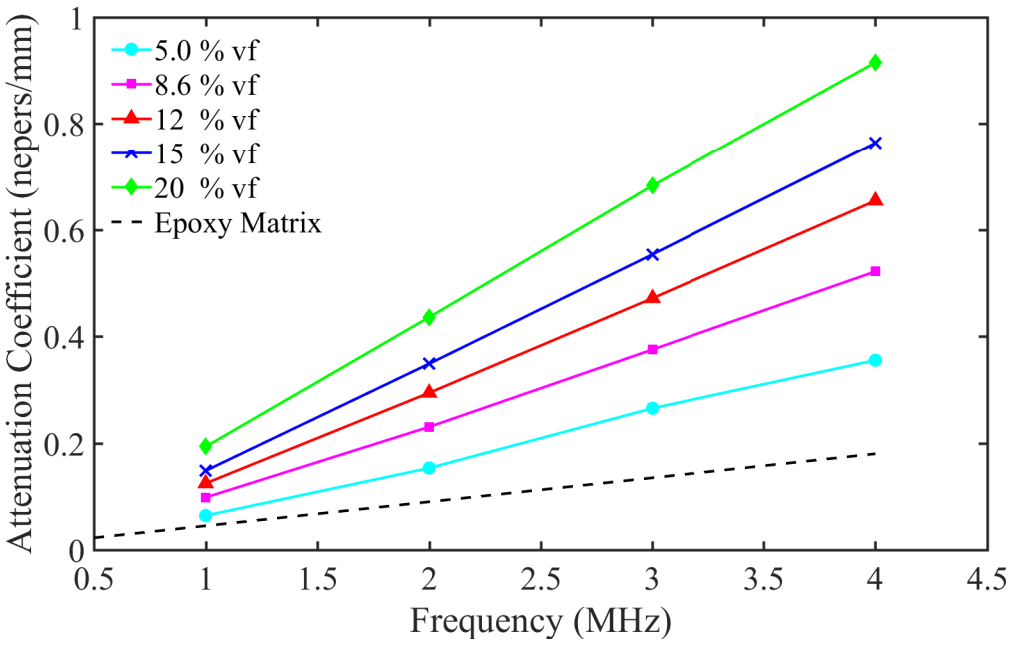

Figure 5.7: Effect of loading frequency on attenuation for a radius of 120 μm for different volume fractions.

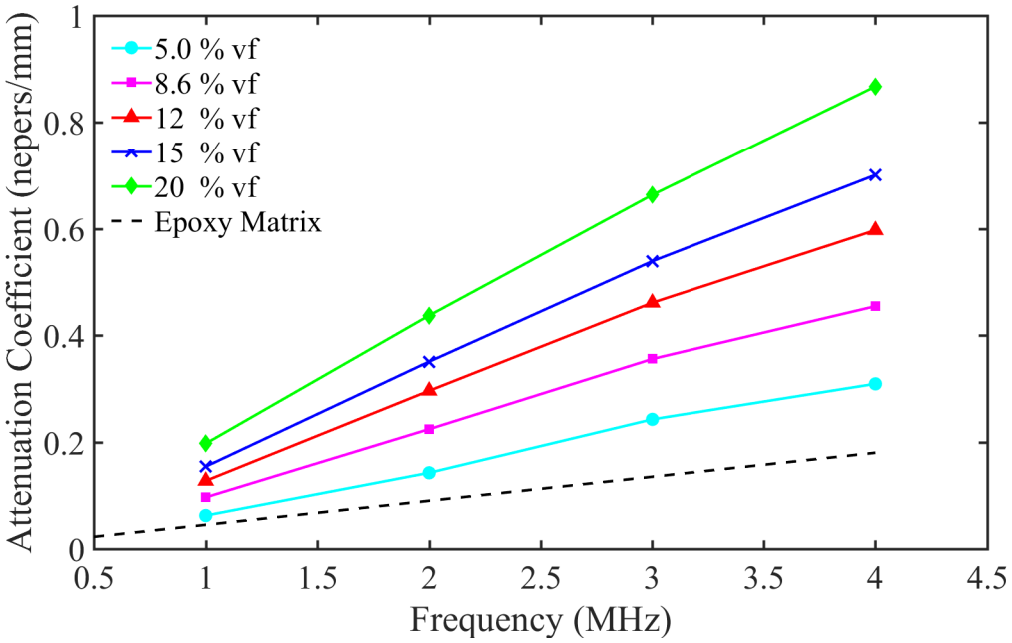

Figure 5.8: Effect of loading frequency on attenuation for a radius of 150 μm for different volume fractions.

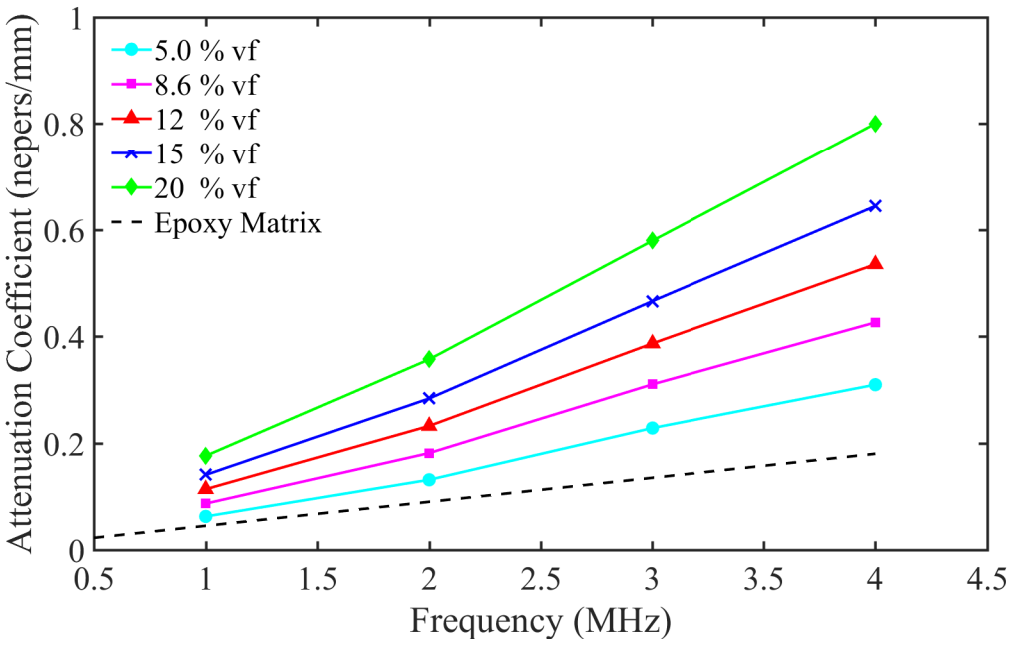

Figure 5.9: Effect of loading frequency on attenuation for a radius of 180 μm for different volume fractions.

Table 5.1: Number of inclusions required at various radii to satisfy the 12% volume fraction.

Radius (μm)	Number of inclusions
120	25
150	13
180	7

5.5 Effect of size of inclusions

Finite element simulations were performed to study the effect of size of inclusions. For this study, finite element models were generated by varying the radius of the inclusions for the same volume fraction. The simulations are carried for inclusions with radius 120 μm, 150 μm, and 180 μm respectively.

The surface area of the inclusions for the finite element models with smaller radius is more as more number of inclusions will be required to achieve the required volume fraction as compared to the number of inclusions required for a model with larger

radius of inclusions as shown in Table 5.1. This increase in surface area results in more scattering of the wave. These scattering will affect the input wave amplitude because more stresses will be dissipated giving rise to more wave attenuation.

The results for this study are shown in Figure 5.10. It can be seen that as the radius of inclusion increases the attenuation characteristics of the polymer composite decreases. The effect gets more pronounced at higher volume fractions as less number of inclusions are required for larger radius of inclusions. This proves that the number of inclusions play an important role in improving the attenuation characteristics of the polymer composite.

5.6 Effect of interphase properties

Interphase properties play an important role in the wave attenuation characteristics of a polymer composite. In order to quantify the effect of the interphase layer on the wave attenuation characteristics of the polymer composite, the sensitivity analysis was performed as described in Section 4.3.2.

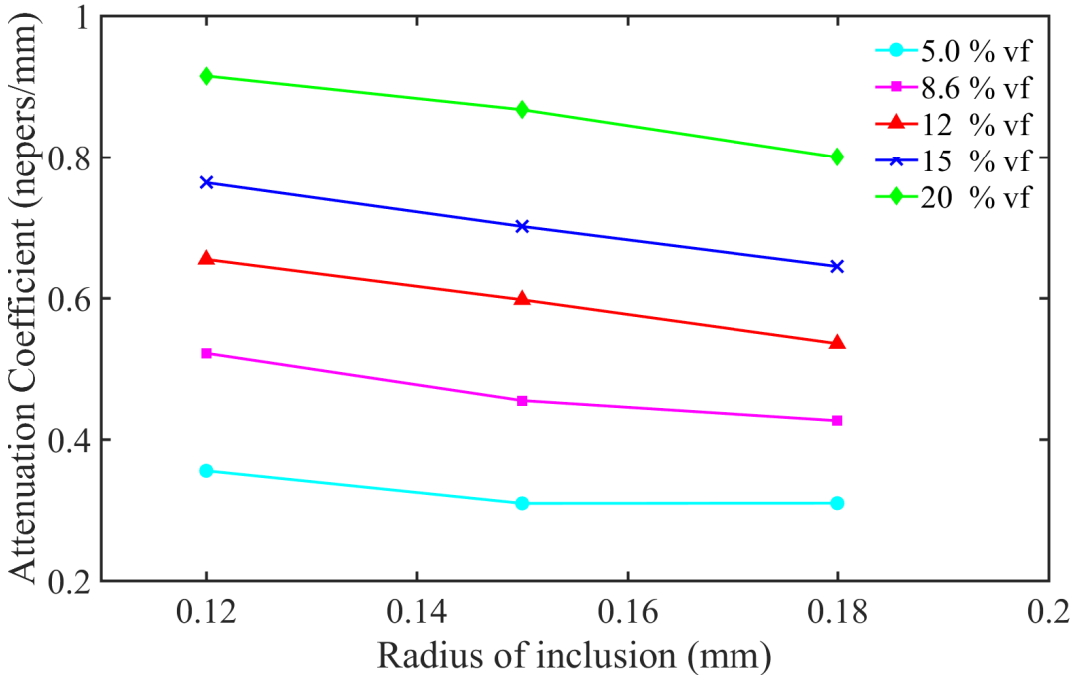

Figure 5.10: Effect of size of inclusions on attenuation characteristics of a polymer composite.

Polynomial regression is a type of regression analysis in which the relationship between the independent variable x and the dependent variable y is modeled as an nth degree polynomial in x. Considering a linear regression, the estimated regression line is defined as [43]:

$$\hat{y} = \hat{\beta}_0 + \hat{\beta}_1 x \tag{5.2}$$

where $\hat{\beta}_0$ and $\hat{\beta}_1$ defined as:

$$\hat{\beta}_0 = \bar{y} - \hat{\beta}_1 \bar{x}, \qquad \hat{\beta}_1 = \frac{S_{xy}}{S_{xx}}, \qquad S_{xx} = \sum_{i=1}^{n} x_i^2 - n\bar{x}^2, \qquad S_{xy} = \sum_{i=1}^{n} y_i x_i - n\bar{x}\bar{y} \tag{5.3}$$

In Eq 5.3, x_i and y_i are inputs and outputs, $\bar{x}$ and $\bar{y}$ are mean values of the inputs and outputs and n is the number of observations. Coefficients $\hat{\beta}_0$ and $\hat{\beta}_1$ are the intercept and the slope of the regression line respectively. The linear regression model was used to compute the intercept ($\hat{\beta}_0$) and slope ($\hat{\beta}_1$) of regression line for different frequencies and volume fractions. The intercept and the slope for the linear regression model are listed in Table 5.2 and 5.3 respectively for 5% volume fraction. The intercept and the slope values for the linear regression model for 8.6% volume fraction are listed in Table 5.4 and 5.5 respectively.

The results for 5% volume fraction from the Table 5.2 show that the slope and the intercept of the linear regression model increase as the loading frequency increases and the slope always remains positive. This shows that for higher frequencies, composites having stiffer interphases exhibit higher attenuation characteristics. The intercept also increases confirming that at higher frequencies the attenuation characteristics of the polymer composite are better than those at lower frequencies. Similar results are observed for 8.6% volume fraction which are shown in Table 5.4.

In a similar manner, the results for 5% volume fraction from the Table 5.3 show that both the intercept and slope of the linear regression model increase as the frequency increases and the slope always remains positive. It can be inferred from these results

Table 5.2: The intercept and slope of linear regression models for attenuation coefficient (α) of polymer composite versus Young's modulus of the interphase for 5 % volume fraction.

Loading frequency (MHz)	1	2	3	4
Intercept ($\hat{\beta}_0$)	0.0699	0.1591	0.2443	0.3804
Slope $\times 10^{-7}$ ($\hat{\beta}_1$)	0.3287	1.2079	1.5012	4.2883

Table 5.3: The intercept and slope of linear regression model for attenuation coefficient (α) of polymer composite versus thickness of the interphase for 5 % volume fraction.

Loading frequency (MHz)	1	2	3	4
Intercept ($\hat{\beta}_0$)	0.0568	0.1227	0.1647	0.2703
Slope ($\hat{\beta}_1$)	0.6299	1.7898	3.7514	5.5106

Table 5.4: The intercept and slope of linear regression models for attenuation coefficient (α) of polymer composite versus Young's modulus of the interphase for 8.6% volume fraction.

Loading frequency (MHz)	1	2	3	4
Intercept ($\hat{\beta}_0$)	0.1057	0.2324	0.3943	0.5858
Slope $\times 10^{-7}$ ($\hat{\beta}_1$)	0.7348	1.5631	4.2142	8.8130

Table 5.5: The intercept and slope of linear regression model for attenuation coefficient (α) of polymer composite versus thickness of the interphase for 8.6% volume fraction.

Loading frequency (MHz)	1	2	3	4
Intercept ($\hat{\beta}_0$)	0.0907	0.1791	0.2768	0.4547
Slope ($\hat{\beta}_1$)	0.7720	2.5951	5.8269	7.0916

that for a given thickness of the interphase, the polymer composite shows higher attenuation characteristics at higher frequencies than that at lower frequencies. The increase in the value of the intercept confirms that the attenuation characteristics are better at higher frequencies than that at lower frequencies. Similar results are obtained for 8.6% volume fraction which can be seen in Table 5.5.

Figures 5.11 - 5.14 show the scatter plot of the attenuation coefficient (α) versus

the (a) Young's modulus of the interphase region and (b) the interphase thickness for 5% volume fraction and Figures 5.15 - 5.18 show the same scatter plot for 8.6% volume fraction. The x-axis is used to show the scale of two independent variables, the Young's modulus (E_i) of the interphase region and the interphase thickness (t_i) and y-axis measure the attenuation coefficient (α) as the dependent variable. The figures also show the regions with 95% Confidence Intervals (CIs) and 95% Prediction Intervals (PIs). The area which lies between the red lines depicts the 95% CIs while the 95% PIs are depicted by the area between the magenta lines. The bounds of the regression function that can be expected are depicted by the confidence interval lines, while the width of the confidence interval provides an indication of the quality of the fitted regression function. The likely location of the true population parameter can be inferred from the CIs, while the PIs can be used to determine the distribution of values and where the next data point can be expected. The width of the prediction interval is always wider than the CIs as the PIs takes into consideration the uncertainty in knowing te value of the population as well as the data scatter.

5.6.1 Comparison of results for with and without interphase

The Figure 5.19 shows the wave attenuation characteristics of a polymer composite with radius of inclusion 150μm for two cases, (a) no interphase between the inclusion and the polymer matrix and (b) interphase between the inclusion and the polymer matrix. The results are shown for 5% and 8.6% volume fraction for both the cases respectively. The results for the case (b) are plotted using Young's modulus as 33.003 GPa and thickness as 12.5% of radius. As can be seen from the Figure 5.19 the presence of interphase affects the attenuation characteristics of the wave. The difference between the two cases are minimal at lower frequencies while a considerable difference is seen at higher frequencies. Thus, we can conclude that interphase properties play an important role in the attenuation characteristics of the polymer composite and should be considered for studies involving attenuation characteristics for the polymer

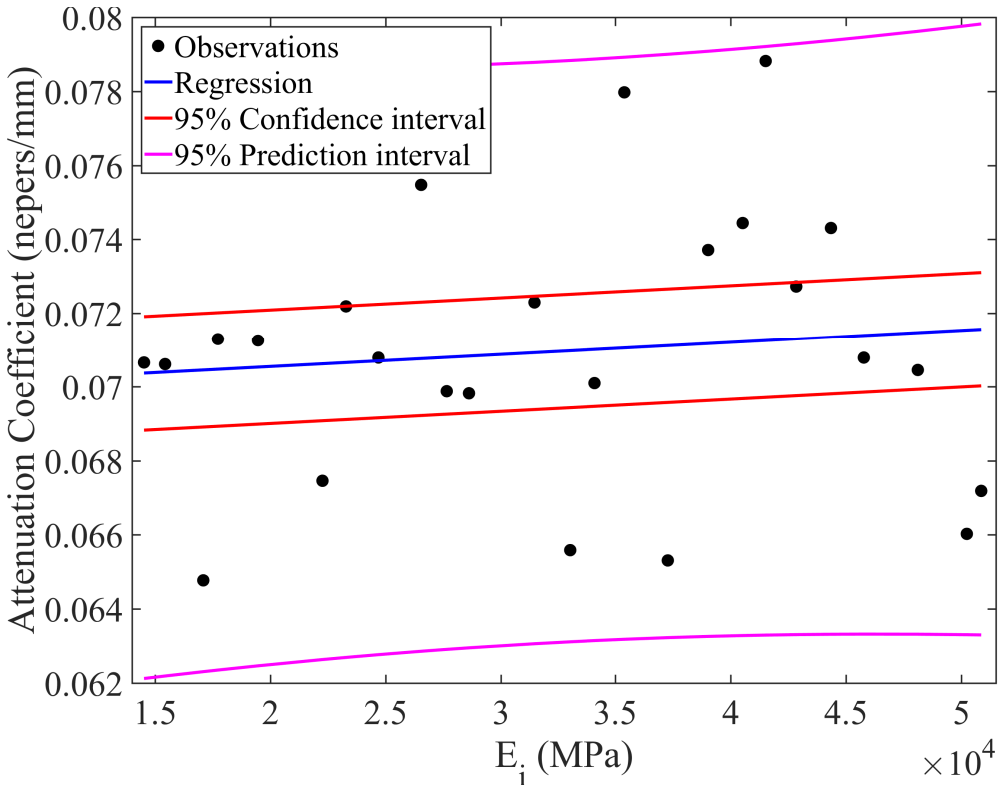

(a)

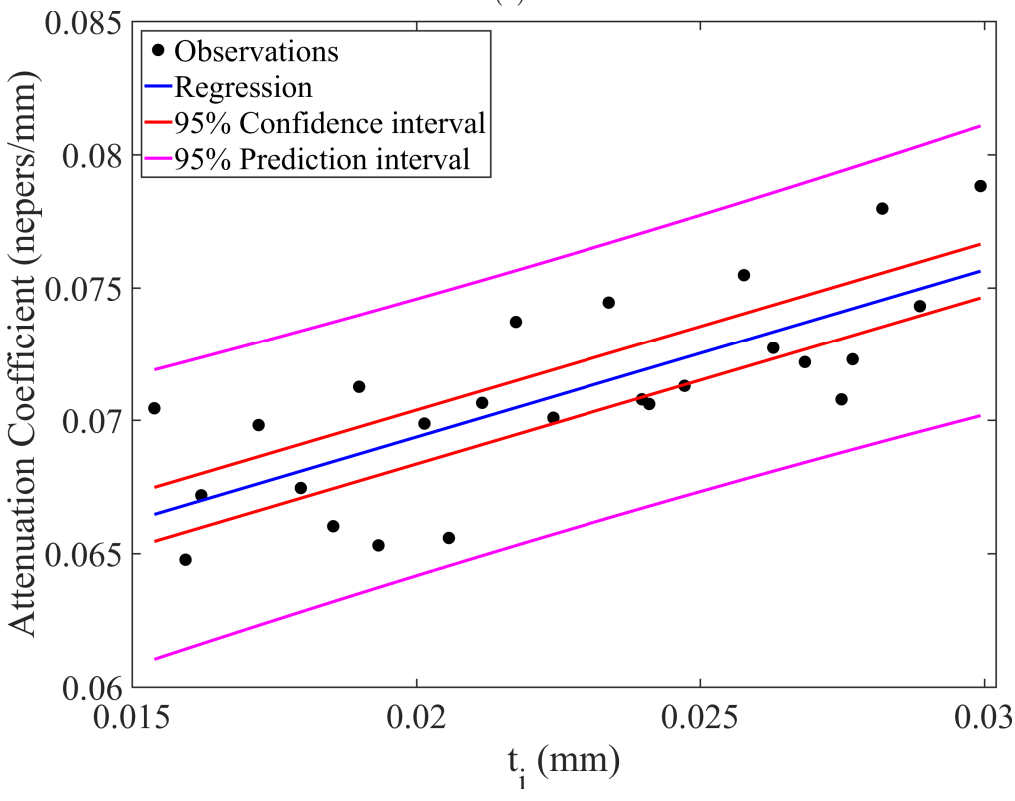

(b)

Figure 5.11: The attenuation co-efficient (α) of 5 % glass-epoxy composite versus (a) Young's Modulus and (b) thickness of interphase region for loading frequency 1 MHz.

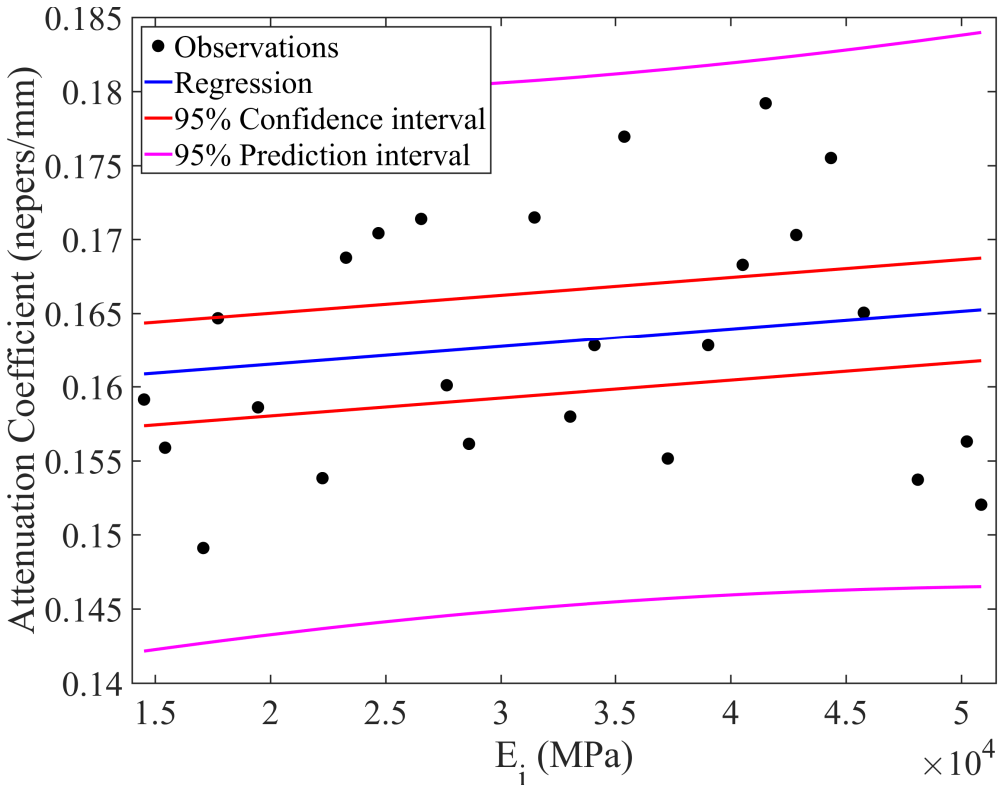

(a)

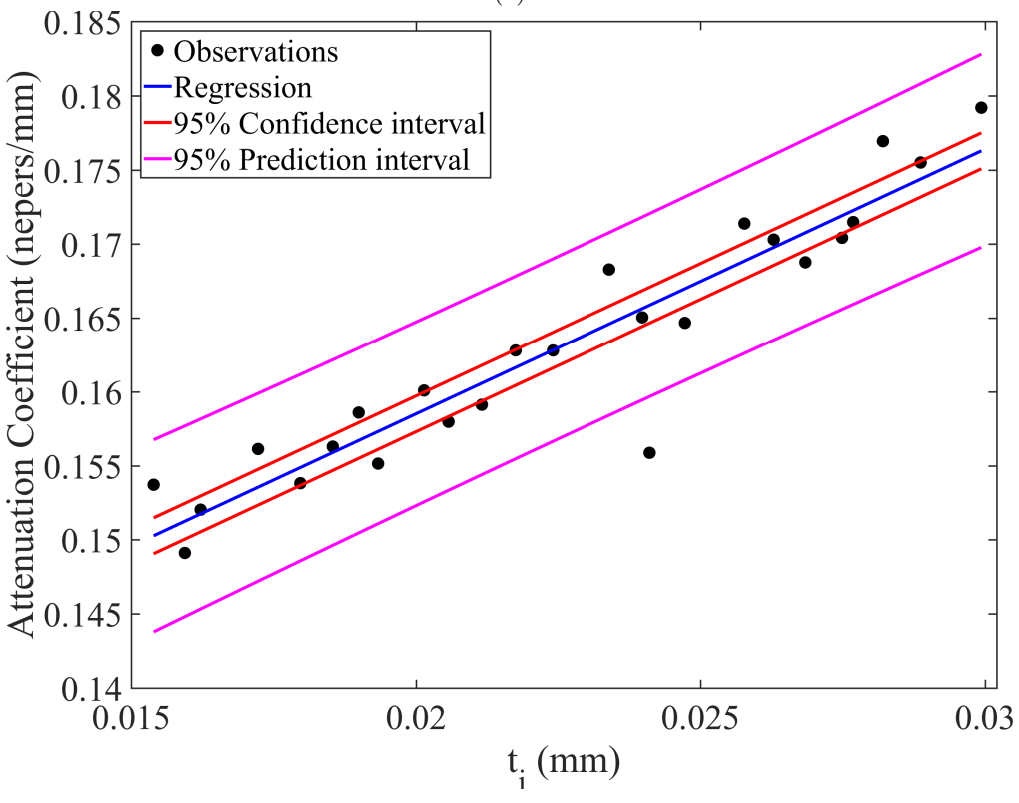

(b)

Figure 5.12: The attenuation co-efficient (α) of 5 % glass-epoxy composite versus (a) Young's Modulus and (b) thickness of interphase region for loading frequency 2 MHz.

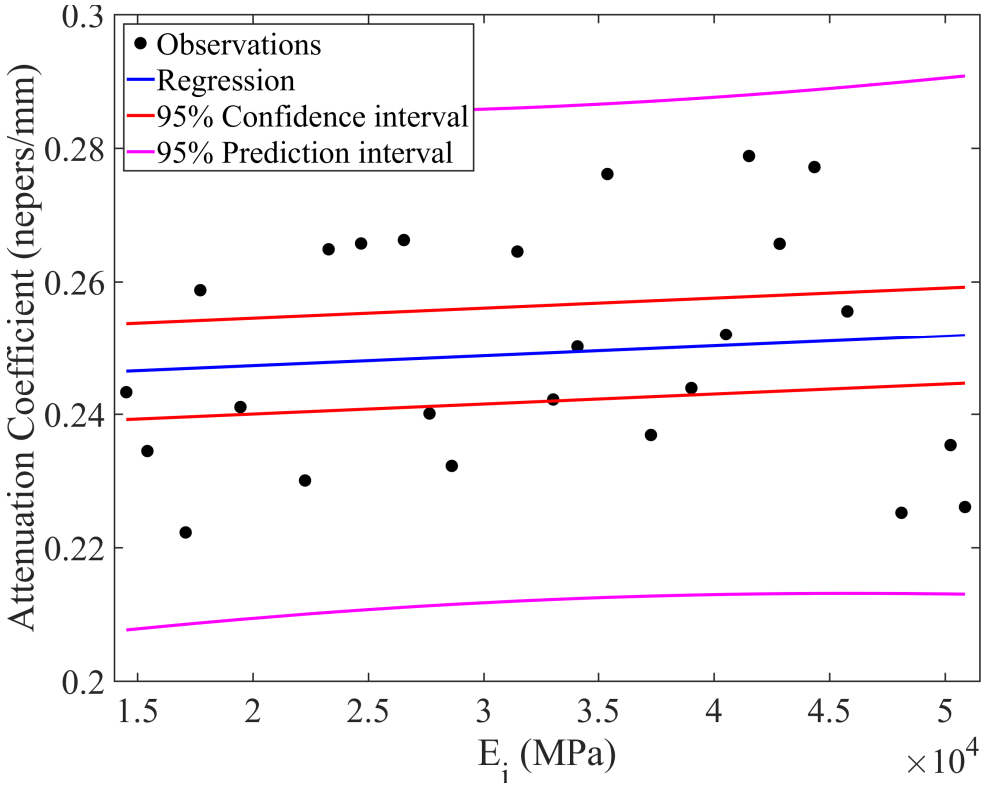

(a)

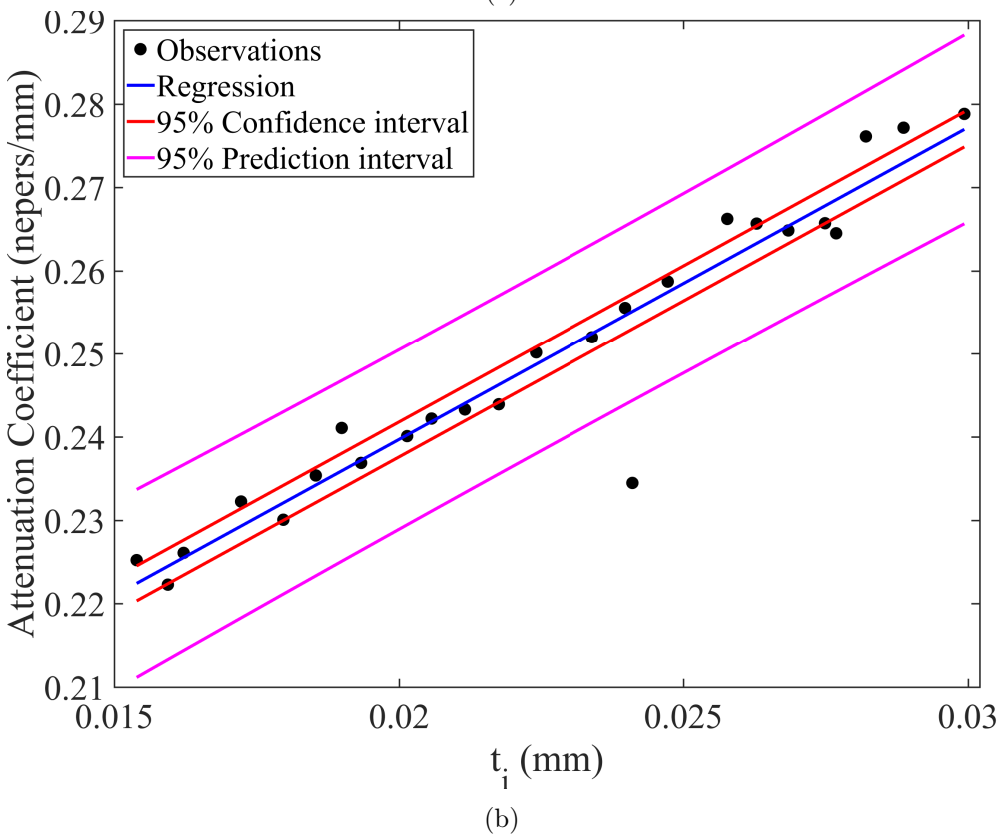

(b)

Figure 5.13: The attenuation co-efficient (α) of 5 % glass-epoxy composite versus (a) Young's Modulus and (b) thickness of interphase region for loading frequency 3 MHz.

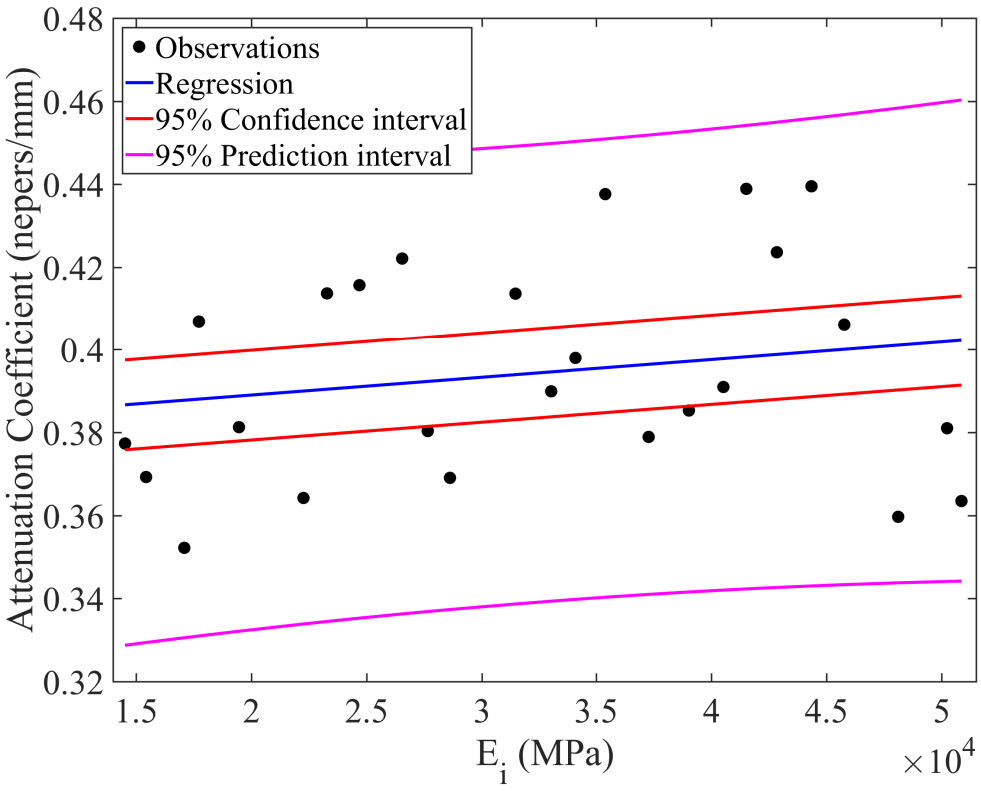

(a)

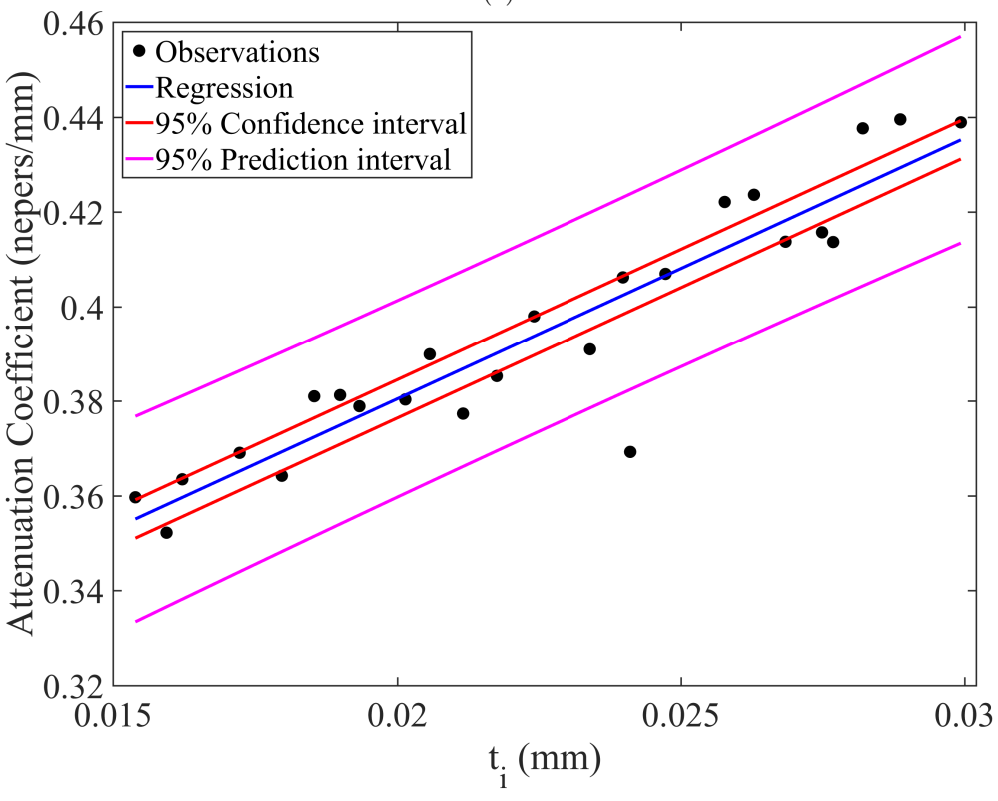

(b)

Figure 5.14: The attenuation co-efficient (α) of 5 % glass-epoxy composite versus (a) Young's Modulus and (b) thickness of interphase region for loading frequency 4 MHz.

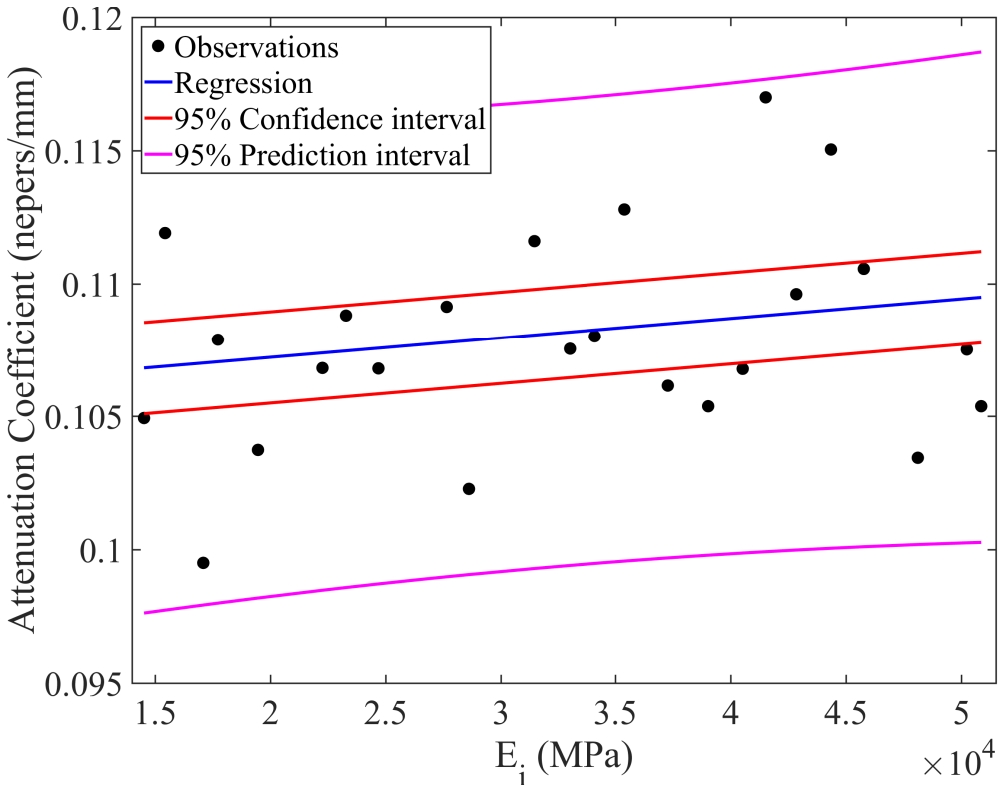

(a)

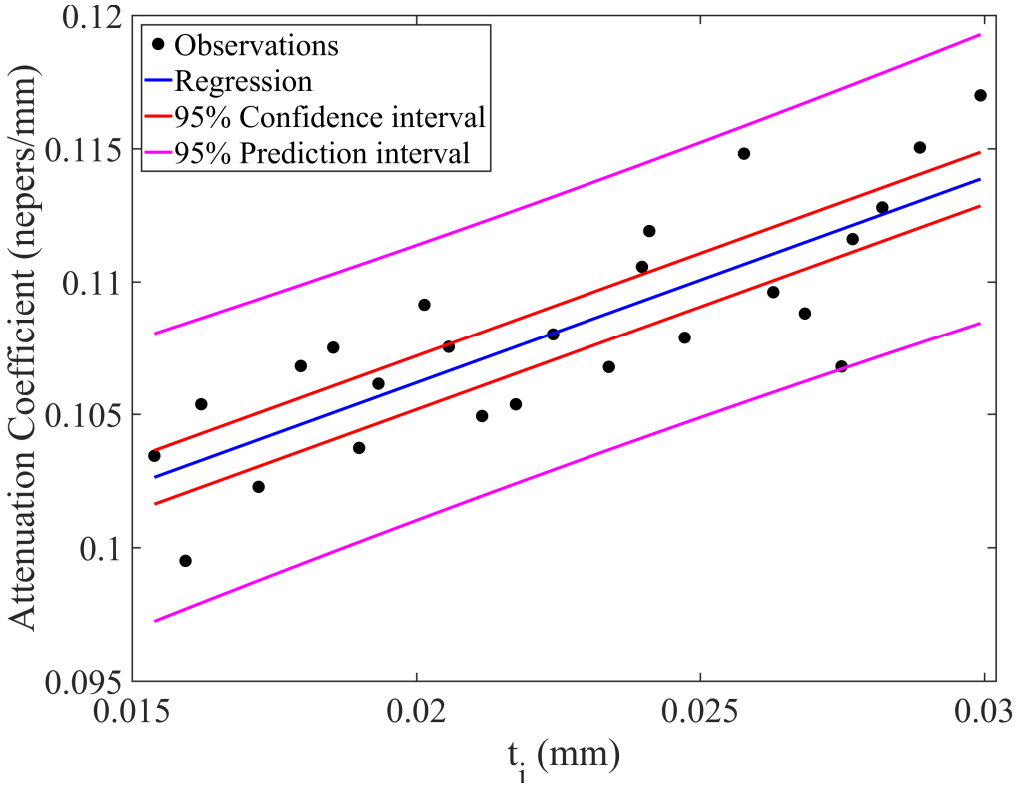

(b)

Figure 5.15: The attenuation co-efficient (α) of 8.6 % glass-epoxy composite versus (a) Young's Modulus and (b) thickness of interphase region for loading frequency 1 MHz.

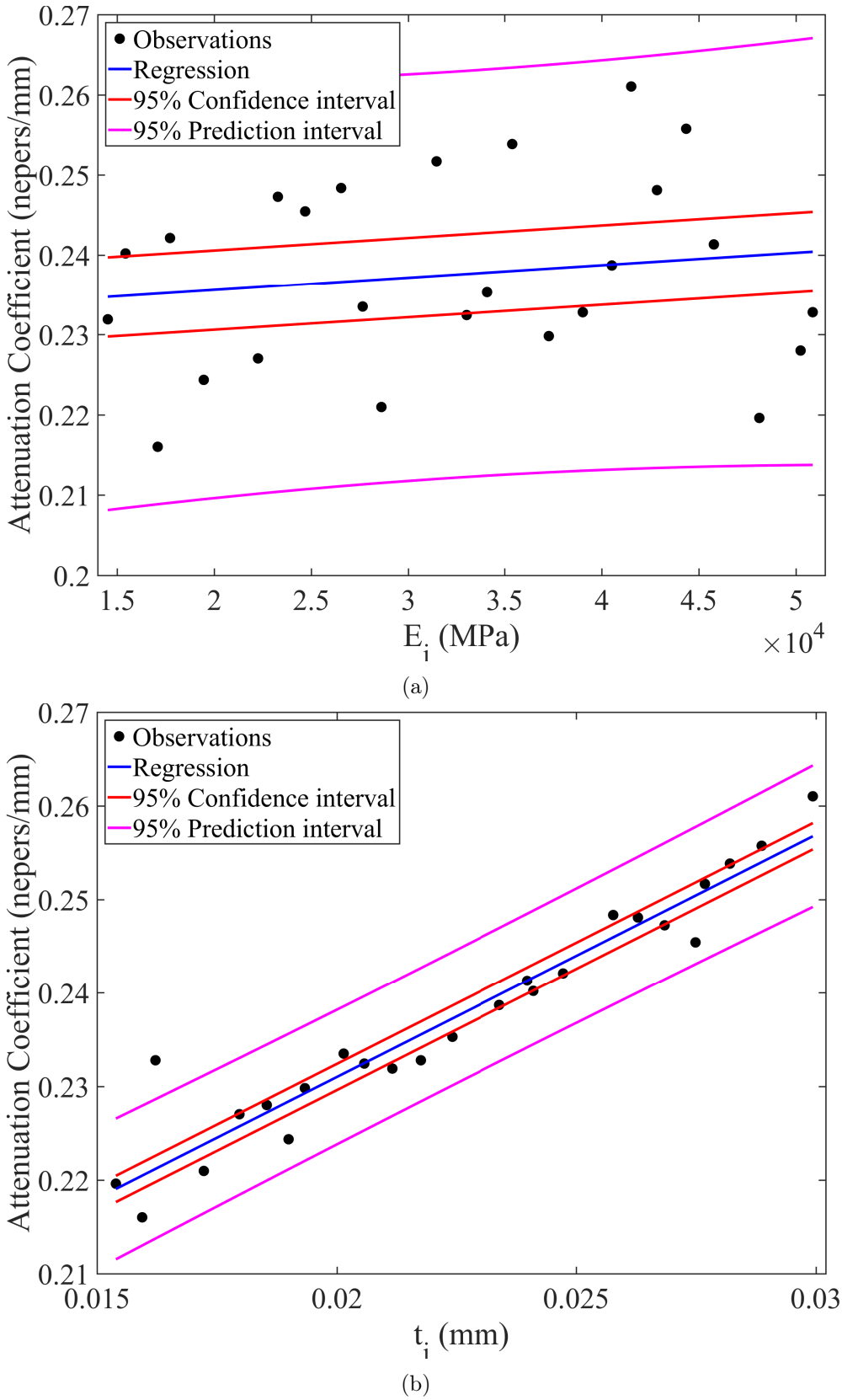

Figure 5.16: The attenuation co-efficient (α) of 8.6 % glass-epoxy composite versus (a) Young's Modulus and (b) thickness of interphase region for loading frequency 2 MHz.

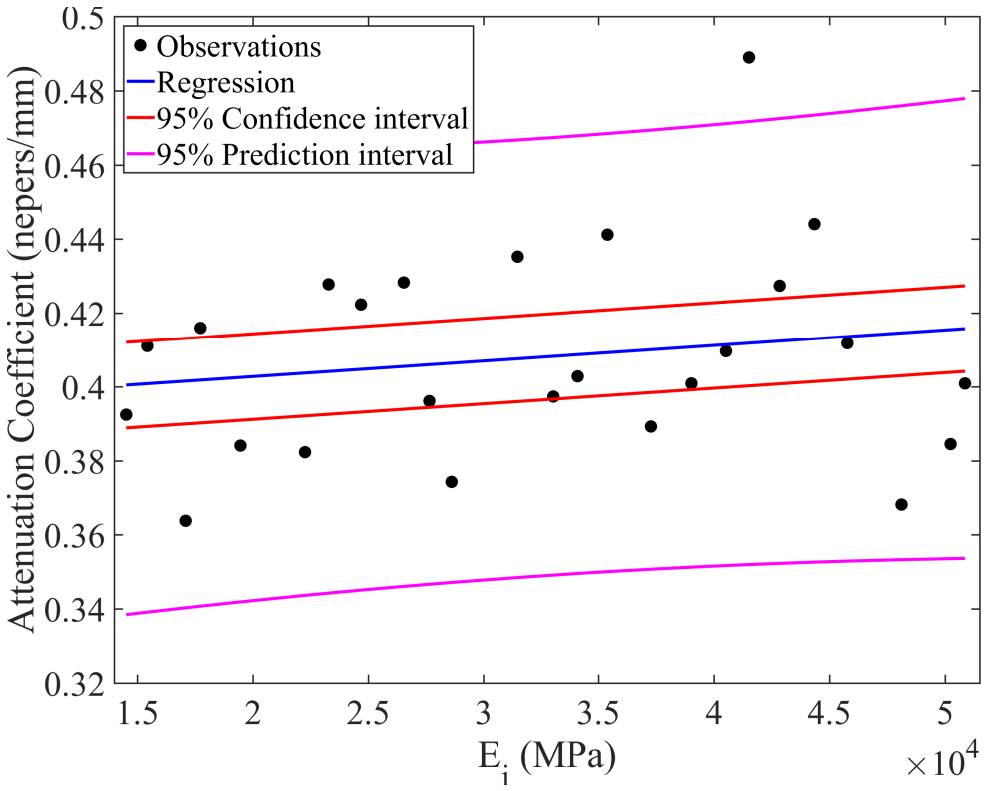

(a)

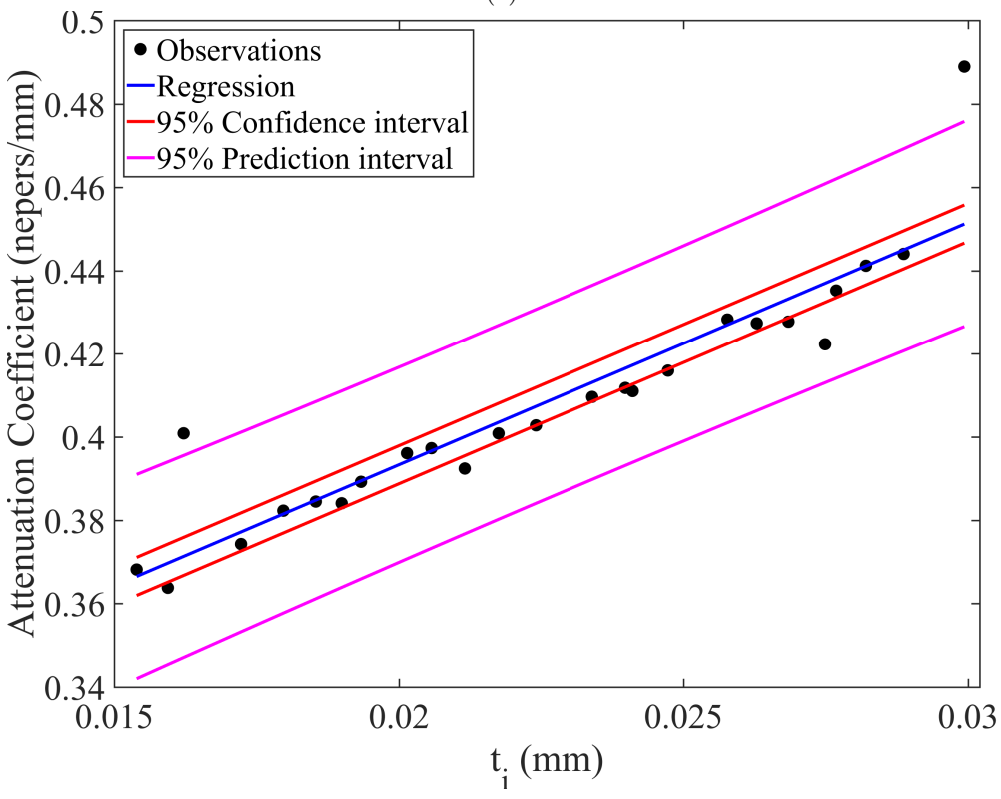

(b)

Figure 5.17: The attenuation co-efficient (α) of 8.6 % glass-epoxy composite versus (a) Young's Modulus and (b) thickness of interphase region for loading frequency 3 MHz.

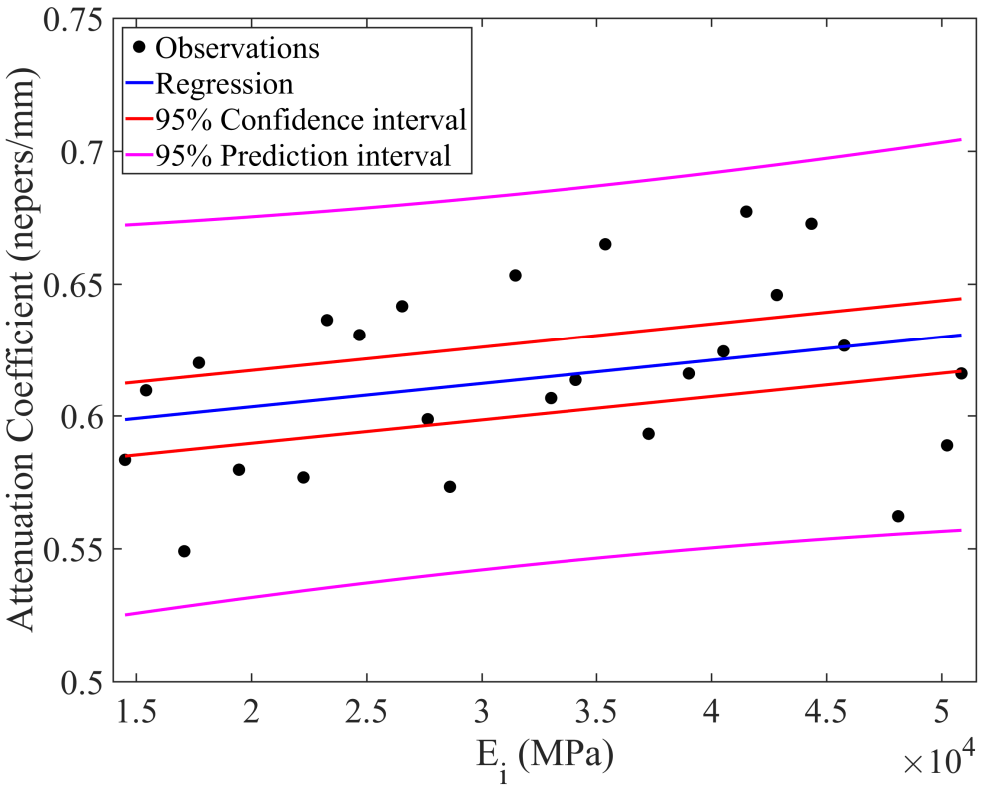

(a)

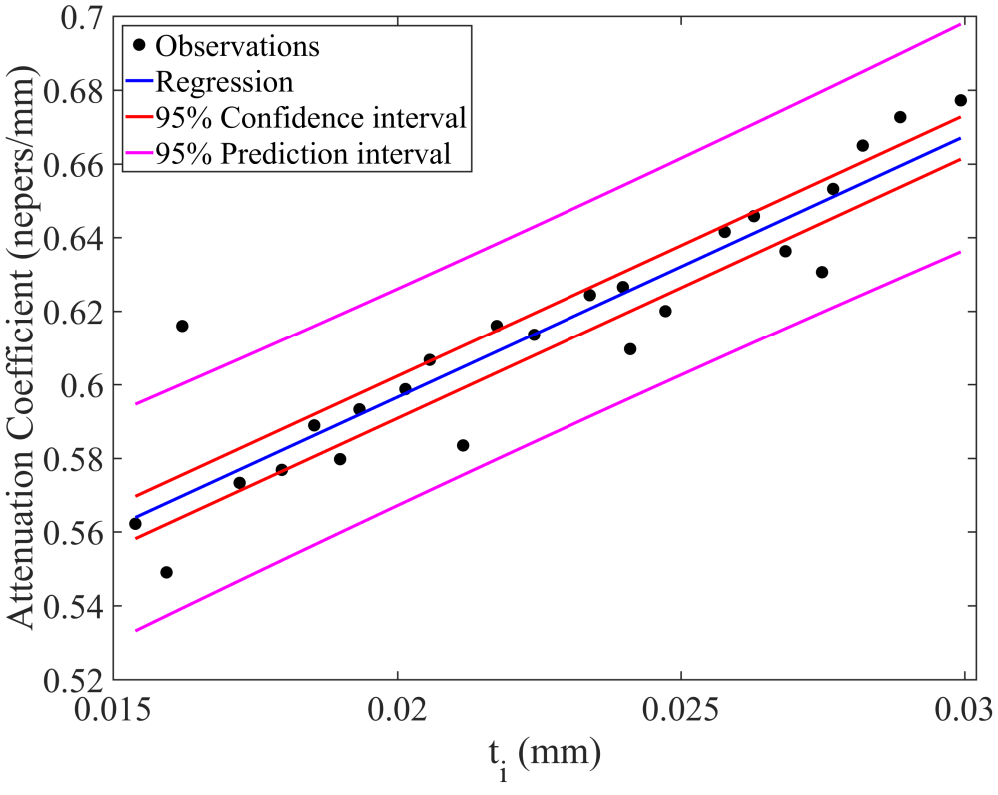

(b)

Figure 5.18: The attenuation co-efficient (α) of 8.6 % glass-epoxy composite versus (a) Young's Modulus and (b) thickness of interphase region for loading frequency 4 MHz.

composite.

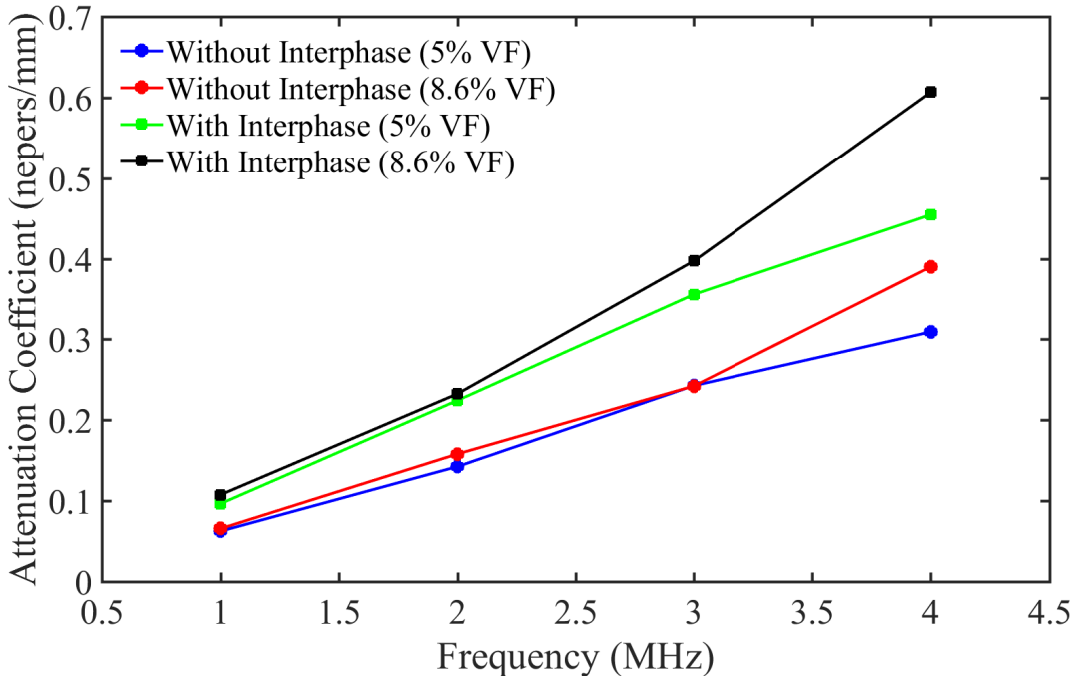

Figure 5.19: Comparison of results for a polymer composite with and without interphase for the inclusions.

5.6.2 Comparison of results for different volume fractions

Figures 5.20 and 5.21 show the attenuation coefficient at 5% and 8.6% volume fraction against the Young's modulus of the interphase. As can be seen from Table

Table 5.6: Comparison of attenuation coefficient at 5% and 8.6% volume fraction against the Young's Modulus of the interphase for loading frequency of 1 MHz.

Volume Fraction (%)	5	8.6
Intercept ($\hat{\beta}_0$)	0.0699	0.1057
Slope $\times 10^{-7}$ ($\hat{\beta}_1$)	0.3287	0.7348

Table 5.7: Comparison of attenuation coefficient at 5% and 8.6% volume fraction against the Young's Modulus of the interphase for loading frequency of 4 MHz.

Volume Fraction (%)	5	8.6
Intercept ($\hat{\beta}_0$)	0.3804	0.5858
Slope $\times 10^{-7}$ ($\hat{\beta}_1$)	4.2883	8.8130

5.6 as the volume fraction is increased the slope of the regression line also increases indicating that at higher volume fraction higher attenuation is observed. Similar results are observed for when the loading frequency is 4 MHz as shown in Table 5.7. This holds true as for higher volume fraction there are more number of inclusions and hence more surface area resulting in more attenuation.

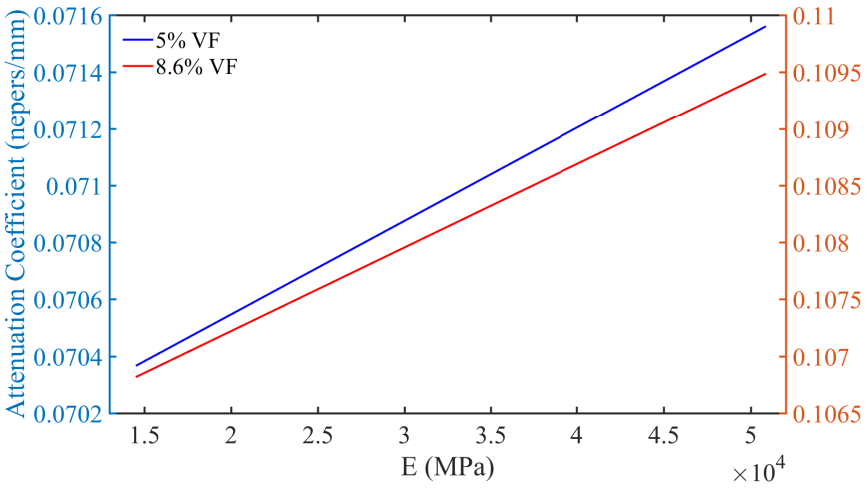

Figure 5.20: Comparison of results for 5% and 8.6% volume fraction for loading frequency of 1 MHz.

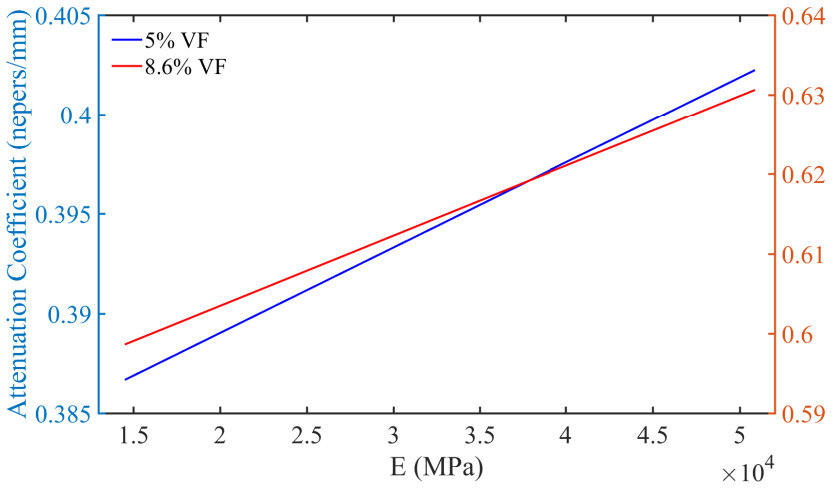

Figure 5.21: Comparison of results for 5% and 8.6% volume fraction for loading frequency of 4 MHz.

CHAPTER 6: CONCLUSION

From the results and discussions from the preceding chapters we have seen that the addition of small sized glass inclusions in the epoxy matrix can significantly alter the attenuation characteristics of the polymer matrix composite. The volume fraction and the size of the inclusions also have an important role in the attenuation characteristics of the polymer composite. Other factors which play an important role in the attenuation characteristics of the polymer composites are the loading frequency, properties of the interphase between the inclusions and the polymer matrix.

We have shown that the finite element technique can be used to evaluate the attenuation characteristics of the polymer composite with spherical inclusions. A viscoelastic model was used for the polymer matrix as it would consider the time and strain rate dependence of the properties of polymer matrix as compared to any other constitutive model. Prony series expansion terms can be used to define the stress relaxation for this type of material.

We see that the position of the inclusions in a polymer composite plays an important role in the attenuation characteristics. Thus, ensemble averaging was used to remove the effect of randomness caused by the positioning of the inclusions.

We see that there is a direct relationship between the volume fraction of the inclusions and the attenuation characteristics of the polymer composite. It is observed that as the volume fraction increases the attenuation in the polymer composite also increases. There is negligible attenuation observed in a polymer matrix with no inclusions which infers that the attenuation characteristics depend on the presence of inclusions in the matrix. As the volume fractions increases, the number of inclusions of the same size also increases resulting in more attenuation by scattering of waves

off the inclusion surfaces.

The loading frequency plays an important role in the attenuation characteristics of the polymer composites. It is observed from the results that as the loading frequency was increased there was an increase in the attenuation characteristics of the polymer matrix which was observed more at higher volume fraction of the inclusions.

We also observed that the size of inclusions is a major factor in the attenuation characteristics of a polymer composite. The surface area of the inclusions increases as the volume fraction is increased as more inclusions are added to achieve the volume fraction. This results in more scattering from the surface of the inclusions thereby improving the attenuation characteristics of the polymer composite. But higher number of large inclusions will increase the volume fraction and in turn the weight of the polymer composite as the inclusions are denser than the polymer matrix. Thus, smaller inclusions with high volume fraction would significantly improve the attenuation characteristics of the polymer composite.

We have also seen that the interphase properties like the Young's modulus and the thickness of the interphase have considerable effect on the wave attenuation characteristics of the polymer composites. We compared two cases one in which interphase was studied and the other in which there was no interphase in polymer composite. It was found that the interphase properties do alter the attenuation characteristics of the polymer composites and hence a comprehensive study should be done before they can be used in any applications.

In regards to future work, the scope if this study should be validation by experiments. Studies can also be done by changing the shape of the inclusions like a cylindrical inclusion and evaluate it's effect on the attenuation characteristics of the polymer composite.

REFERENCES

[1] J. Segurado and J. Llorca, "A numerical approximation to the elastic properties of sphere-reinforced composites," *Journal of the Mechanics and Physics of Solids*, vol. 50, no. 10, pp. 2107–2121, 2002.

[2] Z. Liu, J. Oswald, and T. Belytschko, "Xfem modeling of ultrasonic wave propagation in polymer matrix particulate/fibrous composites," *Wave Motion*, vol. 50, no. 3, pp. 389–401, 2013.

[3] S. Biwa, S. Idekoba, and N. Ohno, "Wave attenuation in particulate polymer composites: independent scattering/absorption analysis and comparison to measurements," *Mechanics of materials*, vol. 34, no. 10, pp. 671–682, 2002.

[4] S. Rokhlin, D. Lewis, K. Graff, and L. Adler, "Real-time study of frequency dependence of attenuation and velocity of ultrasonic waves during the curing reaction of epoxy resin," *The Journal of the Acoustical Society of America*, vol. 79, no. 6, pp. 1786–1793, 1986.

[5] S. Baudouin and B. Hosten, "Immersion ultrasonic method to measure elastic constants and anisotropic attenuation in polymer-matrix and fiber-reinforced composite materials," *Ultrasonics*, vol. 34, no. 2-5, pp. 379–382, 1996.

[6] S. Biwa, Y. Watanabe, and N. Ohno, "Modelling of ultrasonic attenuation in unidirectional fiber reinforced plastics," *Nondestructive Characterization of Materials*, vol. 10, pp. 223–230, 2001.

[7] S. Biwa, N. Ito, and N. Ohno, "Elastic properties of rubber particles in toughened pmma: ultrasonic and micromechanical evaluation," *Mechanics of materials*, vol. 33, no. 12, pp. 717–728, 2001.

[8] J.-Y. Kim, "Models for wave propagation in two-dimensional random composites: A comparative study," *The Journal of the Acoustical Society of America*, vol. 127, no. 4, pp. 2201–2209, 2010.

[9] P. C. Waterman and R. Truell, "Multiple scattering of waves," *Journal of Mathematical Physics*, vol. 2, no. 4, pp. 512–537, 1961.

[10] P. Lloyd and M. Berry, "Wave propagation through an assembly of spheres: Iv. relations between different multiple scattering theories," *Proceedings of the Physical Society*, vol. 91, no. 3, p. 678, 1967.

[11] V. K. Varadan, V. V. Varadan, and Y.-H. Pao, "Multiple scattering of elastic waves by cylinders of arbitrary cross section. i. sh waves," *The Journal of the Acoustical Society of America*, vol. 63, no. 5, pp. 1310–1319, 1978.

[12] S. Kanaun and V. Levin, "Effective medium method in the problem of axial elastic shear wave propagation through fiber composites," *International journal of solids and structures*, vol. 40, no. 18, pp. 4859–4878, 2003.

[13] F. J. Sabina and J. Willis, "A simple self-consistent analysis of wave propagation in particulate composites," *Wave motion*, vol. 10, no. 2, pp. 127–142, 1988.

[14] J.-Y. Kim, "Dynamic self-consistent analysis for elastic wave propagation in fiber reinforced composites," *The Journal of the Acoustical Society of America*, vol. 100, no. 4, pp. 2002–2010, 1996.

[15] A. I. Beltzer and N. Brauner, "The dynamic response of random composites by a causal differential method," *Mechanics of Materials*, vol. 6, no. 4, pp. 337–345, 1987.

[16] R.-B. Yang and A. K. Mal, "Multiple scattering of elastic waves in a fiber-reinforced composite," *Journal of the Mechanics and Physics of Solids*, vol. 42, no. 12, pp. 1945–1968, 1994.

[17] V. K. Kinra, M. S. Petraitis, and S. K. Datta, "Ultrasonic wave propagation in a random particulate composite," *International Journal of Solids and Structures*, vol. 16, no. 4, pp. 301–312, 1980.

[18] S. D. Gardner, C. U. Pittman JR, and R. M. Hackett, "Residual thermal stresses in filamentary polymer-matrix composites containing an elastomeric interphase," *Journal of composite materials*, vol. 27, no. 8, pp. 830–860, 1993.

[19] G. Papanicolaou, G. Messinis, and S. Karakatsanidis, "The effect of interfacial conditions on the elastic-longitudinal modulus of fibre reinforced composites," *Journal of materials science*, vol. 24, no. 2, pp. 395–401, 1989.

[20] P. Theocaris, "The unfolding model for the representation of the mesophase layer in composites," *Journal of Applied Polymer Science*, vol. 30, no. 2, pp. 621–645, 1985.

[21] J.-K. Kim and A. Hodzic, "Nanoscale characterisation of thickness and properties of interphase in polymer matrix composites," *The Journal of Adhesion*, vol. 79, no. 4, pp. 383–414, 2003.

[22] L. S. Schadler, S. K. Kumar, B. C. Benicewicz, S. L. Lewis, and S. E. Harton, "Designed interfaces in polymer nanocomposites: A fundamental viewpoint," *MRS bulletin*, vol. 32, no. 04, pp. 335–340, 2007.

[23] T. Ohji, T. Hirano, A. Nakahira, and K. Niihara, "Particle/matrix interface and its role in creep inhibition in alumina/silicon carbide nanocomposites," *Journal of the American Ceramic Society*, vol. 79, no. 1, pp. 33–45, 1996.

[24] B. Pukánszky, "Interfaces and interphases in multicomponent materials: past, present, future," *European Polymer Journal*, vol. 41, no. 4, pp. 645–662, 2005.

[25] M. Roy, J. Nelson, R. MacCrone, L. S. Schadler, C. Reed, and R. Keefe, "Polymer nanocomposite dielectrics-the role of the interface," *IEEE Transactions on Dielectrics and Electrical Insulation*, vol. 12, no. 4, pp. 629–643, 2005.

[26] "Ds simulia corp., abaqus 6.13 theory manual,"

[27] J. Feder, "Random sequential adsorption," *Journal of Theoretical Biology*, vol. 87, no. 2, pp. 237–254, 1980.

[28] S. Kari, H. Berger, and U. Gabbert, "Numerical evaluation of effective material properties of randomly distributed short cylindrical fibre composites," *Computational Materials Science*, vol. 39, no. 1, pp. 198–204, 2007.

[29] Y. Pan, L. Iorga, and A. A. Pelegri, "Numerical generation of a random chopped fiber composite rve and its elastic properties," *Composites Science and Technology*, vol. 68, no. 13, pp. 2792–2798, 2008.

[30] M. Silani, H. Talebi, S. Ziaei-Rad, P. Kerfriden, S. P. Bordas, and T. Rabczuk, "Stochastic modelling of clay/epoxy nanocomposites," *Composite Structures*, vol. 118, pp. 241–249, 2014.

[31] A. A. Gusev, "Representative volume element size for elastic composites: a numerical study," *Journal of the Mechanics and Physics of Solids*, vol. 45, no. 9, pp. 1449–1459, 1997.

[32] A. Gusev, M. Heggli, H. R. Lusti, and P. J. Hine, "Orientation averaging for stiffness and thermal expansion of short fiber composites," *Advanced Engineering Materials*, vol. 4, no. 12, pp. 931–933, 2002.

[33] M. Schneider, "The sequential addition and migration method to generate representative volume elements for the homogenization of short fiber reinforced plastics," *Computational Mechanics*, pp. 1–17, 2016.

[34] E. Ghossein and M. Lévesque, "Random generation of periodic hard ellipsoids based on molecular dynamics: A computationally-efficient algorithm," *Journal of Computational Physics*, vol. 253, pp. 471–490, 2013.

[35] V. Salnikov, D. Choï, and P. Karamian-Surville, "On efficient and reliable stochastic generation of rves for analysis of composites within the framework of homogenization," *Computational Mechanics*, vol. 55, no. 1, pp. 127–144, 2015.

[36] I. Temizer, "Lecture notes micromechanics analysis of heterogeneous materials," *Department of Mechanical Engineering Bilkent University*, 2007.

[37] A. Wineman and K. Rajagopal, *Mechanical Response of Polymers: An Introduction*. Cambridge University Press, 2000.

[38] H. BRINSON and L. C. Brinson, *Polymer engineering science and viscoelasticity*. Springer, 2016.

[39] R. Y. Rubinstein and D. P. Kroese, *Simulation and the Monte Carlo method*, vol. 10. John Wiley & Sons, 2016.

[40] M. D. McKay, R. J. Beckman, and W. J. Conover, "Comparison of three methods for selecting values of input variables in the analysis of output from a computer code," *Technometrics*, vol. 21, no. 2, pp. 239–245, 1979.

[41] D. Huntington and C. Lyrintzis, "Improvements to and limitations of latin hypercube sampling," *Probabilistic Engineering Mechanics*, vol. 13, no. 4, pp. 245–253, 1998.

[42] MATLAB, *9.2.0.556344 (R2017a)*. Natick, Massachusetts: The MathWorks Inc., 2017.

[43] A. Saltelli, M. Ratto, T. Andres, F. Campolongo, J. Cariboni, D. Gatelli, M. Saisana, and S. Tarantola, *Global sensitivity analysis: the primer*. John Wiley & Sons, 2008.